



MINISTRY OF TECHNOLOGY  
AERONAUTICAL RESEARCH COUNCIL  
CURRENT PAPERS

# Ingestion of Debris into Intakes by Vortex Action

by

*D. E. Glenny*

*N. G. T. E. Pyestock*

LIBRARY  
AERONAUTICAL RESEARCH COUNCIL  
SQUADRON

LONDON: HER MAJESTY'S STATIONERY OFFICE

1970

PRICE 12s 0d [48p] NET



U.D.C. No. 621-757:533.697.2:532.527

## Ingestion of debris into intakes by vortex action

- by -

D. E. Glenny  
N.G.T.E. PyestockSUMMARY

The advent of the big high by-pass ratio engines with their inherently large inlet diameters has resulted in engine installations featuring lower ground clearances than hitherto. Under these circumstances the vortex formed beneath the intake during ground running can be an extremely potent means of lifting ground debris into the intake. This Report considers the impulsive lifting of particles over which the vortex core passes both on a theoretical and an experimental basis. Scaling laws are derived to relate model and full-scale tests and experimental evidence is cited to demonstrate their validity. For a given inlet velocity the strength of the vortex, and thus the maximum size of particle that can be lifted, is very much a function of the ambient vorticity, and of the strength of the wind blowing on to the intake. The ability of atmospheric vorticity to vary from one instant to the next leads to some difficulty in specifying the maximum size of particle that the vortex might lift. Nevertheless it seems reasonable on the basis of the evidence submitted that a 6 ft diameter intake operating with the centreline 6 ft above the ground, as is representative of some current projects, would be capable of ingesting spherical pieces of concrete up to 12 in. in diameter. Various methods of reducing ingestion were examined experimentally, and although some undoubtedly decreased the frequency of ingestion none provided an absolute safeguard. However, an operational technique which might ease the ingestion problem involves a progressive throttle opening as the aircraft initially accelerates on take-off so as to achieve as high a value as possible for the ratio of the wind velocity blowing on to the intake to the intake throat velocity.

---

\*Replaces N.G.T.E. Report No. R.307 - A.R.C.31 474

CONTENTS

	<u>Page</u>
1.0 Introduction	4
2.0 Scaling laws	4
3.0 Experimental - objectives and procedure	5
3.1 Apparatus	5
3.2 Experimental procedure	5
4.0 Results	6
4.1 First observations	6
4.2 Non-uniform cross wind	7
4.3 Ingestion thresholds	8
4.4 Sizes of particle ingested	9
4.5 Theoretical approximation of vortex formation using potential flow	10
4.6 Influence of intake diameter	11
5.0 Comparison with other work - and full-scale predictions	11
6.0 The prevention of ingestion	12
7.0 Conclusions	13
References	15

Detachable Abstract Cards

APPENDICES

<u>No.</u>	<u>Title</u>	
I	List of symbols	16
II	Dimensional analysis of particle lifting by ground vortex	18
III	Analysis of particle lifting based on the pressure distribution within a simple vortex	21

ILLUSTRATIONS

<u>Fig. No.</u>	<u>Title</u>
1	General arrangement and nomenclature for intake
2	Comparison between current and proposed jet transports in terms of H/D ratio
3	Particle ingestion rig showing 6 in. diameter intake
4	Typical velocity profile in plane parallel to the ground: $V_C$ at an angle of $55^\circ$ to intake centreline
5	Plan view of intake ingestion rig showing stations for measuring velocity profiles
6	12 in. diameter intake at an $H/D = 1.2$ showing ingestion of 1 in. diameter glass balls
7	General pattern of ingestion for varying cross winds
8	Sample experimental results
9	Ingestion boundaries in terms of $V_C/V_I$ and $V_I^2/gD$
10	Ingestion boundaries in terms of $V_C/V_I$ and $V_I/wD$
11	Variation of ingestion boundaries with respect to cross wind direction
12	Direction of rotation of vortex with respect to cross wind gradient
13	Effect of varying head wind on intake streamline flow
14	Theoretical maximum $V_C/V_I$ for varying H/D ratios
15	Comparison between N.G.T.E., Rolls-Royce and Douglas ingestion zones in terms of H/D and $V_T/V_I$
16	Simplified vortex model and typical velocity distribution

## 1.0 Introduction

The advent of the big high by-pass ratio engines with their inherently large inlet diameters has resulted in engine installations featuring lower ground clearances than hitherto. The ground clearance can be defined non-dimensionally as the height of the inlet centreline above the ground divided by the throat diameter, see Figure 1, and whereas a few years ago this ratio was typically about 2, values of about 1.0 are now proposed. Figure 2 illustrates more dramatically than do these numbers the greatly increased proximity of the intake to the ground and makes clear the enhanced risk of debris ingestion. One mechanism of ingestion stems from the formation during ground running of a vortex linking the ground to the intake capture plane. Tests preceding the present investigation, conducted by Rolls-Royce, had shown that such a vortex was capable of projecting particles in an impulsive manner to heights far exceeding that of the intake. It is with ingestion consequent on the occurrence of this phenomenon that the present Report is particularly concerned.

## 2.0 Scaling laws

In earlier work concerned with the somewhat similar problem involving debris ingestion and recirculation of hot gases<sup>1</sup> the forces in full-scale and model systems were examined to enable "scaling laws" to be derived. A rather similar method was used<sup>2</sup> in an early treatment of the present problem. The parameters governing debris ingestion may alternatively be derived from a classical dimensional analysis of the process, whilst a second alternative is to use the pressure distribution in a simplified vortex to deduce the forces acting on a particle resting on the ground at the vortex foot. These two methods are treated fully in Appendices II and III. Both develop the following "scaling laws" relating full-scale and model tests, and covering not only the conditions under which vortex ingestion can occur, but also the sizes of particle that can be lifted.

- (1) Particle size is proportional to test scale.
- (2) Intake velocity squared is proportional to test scale.
- (3) Ratio of particle density to fluid density is the same for both full-scale and model tests. Thus for tests at both scales in air the particle densities should be the same.
- (4) Ratio of cross wind velocity to intake throat velocity is the same for model and full size tests.
- (5) Ratio of the intake velocity to the product (cross wind velocity gradient  $\times$  intake diameter) is the same for model and full size tests. This dimensionless group is equivalent to the "Rossby number", which is used in the study of geophysical vortices<sup>3</sup>.

### 3.0 Experimental - objectives and procedure

This part of the Report aims to demonstrate the validity of the laws and their use in determining

- (a) the "ingestion thresholds" separating the conditions under which vortex formation can occur from those which are ingestion free,
- (b) the sizes of particle that can be lifted by the vortex.

#### 3.1 Apparatus

An existing suction line was modified to accept intakes having throat diameters of either 6 in. or 12 in. In addition a fine mesh gauze and collector box were installed in the suction line to prevent ingested particles entering the exhausting compressor. A variable height table was used to simulate the ground and to give ratios of intake centreline height to throat diameter ( $H/D$ ) extending from 0.9 to 1.8 for both the 6 in. and 12 in. diameter intakes. Figure 3 shows the layout of the rig.

Ground debris was simulated with particles of spherical shape, both to ensure similarity between experiments, and because of the known aerodynamic characteristics of spheres. Glass beads were in fact used, as their density compares closely with that of granite or concrete, and so conforms with the "scaling laws". 3 mm and 6 mm diameter beads were found convenient for most of the experiments, although as will be described, some larger beads were also used. The beads were partially constrained from rolling by a wire mesh on the ground to prevent any undue movement associated with extremities of the vortex.

The cross wind was provided by a 7 hp fan. The velocity profile and mean velocity were varied by restricting the outlet with wire mesh and throttling the fan inlet. Typical contours of constant wind speed in the vicinity of the intake are shown in Figure 4. The "velocity gradient" in the wind was measured at a position four intake diameters,  $4D$ , from the intake and  $0.75D$  on either side of a line joining the intake to the fan outlet, and at a height above the ground equal to one half the distance between the ground and the lower lip of the intake. This is shown in Figure 5. The measuring station was considered to be far enough away from the intake not to be affected by the vortex motion, yet near enough to be representative of the velocity gradient imposed on the intake. Figure 5 also defines both the velocity gradient and the "Rossby number". The mean cross wind was calculated from the measured velocity profile.

The intake velocity was determined from the intake mass flow which was measured using a British Standard orifice plate.

#### 3.2 Experimental procedure

As mentioned previously the object of the experiment was to determine ingestion thresholds, and thence to specify the most favourable operating

conditions to reduce the possibility of vortex ingestion. To achieve this, and at the same time to reduce the overall workload the following experimental procedure was adopted.

- (1) The 6 in. diameter intake was set up at an  $(H/D) = 0.9$  with numerous 3 mm glass beads placed beneath the intake to simulate ground debris.
- (2) The inlet velocity was adjusted to a minimum value of 150 ft/s, this corresponding according to the scaling laws with a throat velocity of 600 ft/s in an 8 ft diameter intake.
- (3) The cross wind was inclined at  $55^\circ$  to the intake centreline. (This particular inclination was convenient with the very simple apparatus.) Commencing at the highest possible value the wind velocity was slowly reduced until particle pick-up was just initiated. At this point a pitot traverse was made of the cross wind velocity according to the method shown in Figure 5.
- (4) The procedure was repeated for 25 ft/s increments of intake velocity up to a maximum of 350 ft/s or until a point was reached when the cross wind was no longer capable of preventing ingestion.
- (5) Steps 2, 3 and 4 were repeated for different velocity gradients, this being arranged by altering the gauzing at the fan outlet.
- (6) Having completed a range of velocity gradients steps 2, 3, 4 and 5 were repeated for  $(H/D) = 1.1, 1.3, 1.5$  and  $1.8$ .
- (7) The 6 in. diameter intake was replaced by the 12 in. diameter intake at an  $(H/D) = 0.9$  and the 3 mm particles replaced by ones 6 mm diameter. The experiments were then repeated as in 2, 3, 4, 5 and 6 above.
- (8) The complete procedure given above was repeated with the wind arranged to blow exactly head on to the intake.

#### 4.0 Results

##### 4.1 First observations

Initial tests suggested that the velocity gradients in the wind blowing on to the intake exerted an important influence on the formation of the vortex, and thus on the ingestion process. An early observation was that if the experimenter put his hand partly into the wind at some point between the fan outlet and the intake, the vortex became much more intense. This purely qualitative observation was based on the degree of disturbance among the particles on the "ground" and the rate at which they were lifted. In fact under very carefully regulated conditions, which included shutting all



the doors and windows of the large building in which the tests were conducted, and securing a virtually uniform velocity profile in the "wind" from the fan, the vortex could barely be detected.

With all doors and windows shut and zero wind it was found that neither 3 mm or 6 mm glass particles were lifted by either the 6 in. or the 12 in. diameter intake, even when the intake throat velocity was increased to the choking figure. The delicacy of these situations is however emphasized by the observations that merely opening a door, or perhaps the experimenter moving about in the vicinity of the rig, could so upset the balance that a vortex capable of lifting the test particles was immediately formed. Experiment showed the necessity for particle pick-up of a certain minimum, and in fact extremely low velocity gradient in the wind. However, although these observations under tightly controlled laboratory conditions are no doubt of considerable scientific interest, they were not thought particularly relevant to the very different ambient conditions thought likely on an airfield. Therefore they were not investigated further. Similarly outside the scope of the present work is a closely related phenomenon studied by Norbury<sup>4</sup>. In his experiments the intake velocity was sufficiently low for smoke traces to be used to observe the streamline flow, whilst the tests were carried out in a nominally circulation free environment. The interaction of the intake flow with the ground boundary layer initiates a pair of vortices which coalesce as the (H/D) ratio is increased to form a very weak vortex linking the intake to the ground.

#### 4.2 Non-uniform cross wind

Under this heading is considered what is thought in the present context to be the general case, namely vortex ingestion in the presence of appreciable ambient vorticity. The vortex formed under these conditions wanders over the ground in a random manner in the region of the intake. Particles on the ground near the vortex extremities tend to be blown horizontally, and those that bounce can become airborne under the influence of the local air currents. Experimental observation suggests that such particles might well enter adjacent intakes of a multi-engined installation, but that they are less likely to enter the intake associated with the vortex.

Dramatically different in the manner of lifting is the action of the vortex on those particles over which the vortex core passes. With a vortex of sufficient strength these particles are projected violently upwards, as if under the action of an impulsive force. Figure 6 shows a spark photograph of particles being so lifted. As has been noted, it is with this form of vortex ingestion that the present investigation is concerned. In practice it is likely to occur whenever a sufficiently strong vortex passes over a particle, and it seems particularly likely to involve particles which cannot be removed from the vicinity of the intake by horizontal surface winds: thus debris lodged in cracks in runways, or stones embedded in soft earth adjacent to runway edges seem prone to impulsive lifting. Experimental observation shows that by no means all particles so lifted enter the intake. Many fall clear. Some fly very much higher than the intake. With a given throat velocity the wind can be increased sufficiently to blow the vortex away. As the wind is reduced the vortex first appears (as manifest by an agitation among the particles lying on the ground) downwind

from the intake and offset across the wind as shown in the upper diagram of Figure 7. The vortex follows the path shown in the diagram as the wind is gradually reduced, whilst the increasing proximity of the vortex foot to the intake gradually increases the frequency of ingestion. This frequency is at its highest when the vortex reaches the area signified by the small solid circle.

The lower diagram in Figure 7 shows the vortex history as the wind is gradually increased from zero. The initial ground disturbance is quite small, but as the wind increases the vortex shifts slightly as shown to the area signified by a small solid circle, in which debris ingestion is most likely. Further increases in the wind blow the vortex down and somewhat across wind. As this process continues the risk of ingestion is progressively reduced and finally eliminated.

Very similar observations were made with the wind aligned with the intake. In this case however, as would be expected, the foot of the vortex moved under the intake along a line parallel to the wind direction.

#### 4.3 Ingestion thresholds

It will be recalled that the thresholds considered are those dividing conditions under which ingestion occurred from those which were ingestion free.

A few of the extremely large number of separate observations of these thresholds are plotted in Figure 8 in a manner stemming directly from the scaling laws derived in the Appendices. The confusion of the picture needs no emphasis. In fact the apparent lack of pattern results from the inability with the essentially crude apparatus to vary independently the cross wind velocity and the velocity gradient, for if the points are interpolated to enable lines of constant Rossby number to be drawn the very much clearer picture shown in Figure 9 emerges. This correlation, based on over 250 separate observations, is thought gratifying in view of the difficulty in exactly spotting the onset of ingestion and the simple techniques employed. The Figure refers to tests with both the 12 in. diameter and the 6 in. diameter intakes and at the values of  $(H/D)$  shown. The values for the Rossby number were governed by rig limitations. For given values of  $(H/D)$  and  $R_0$  each line represents an ingestion threshold in the sense that above the line is ingestion free, whilst below the line is ingestion prone. Thus, for  $(H/D) = 1.5$  and  $R_0 = 25$ ,  $V_C/V_I$  has to be increased to 0.06 before the ingestion free zone is entered, that is in effect before the vortex is blown away.

Supporting evidence for the validity of the scaling laws, when applied to the prediction of ingestion thresholds, comes from observations of the first formation of the vortex at the two different intake sizes. With  $(H/D)$  equal to 1.3 and  $R_0 = 25$  the vortex was first observed with both the 6 in. and 12 in. intakes when  $V_C/V_I$  equalled 0.8. Similarly with  $(H/D)$  equal to 1.1 the vortex was first noted with both intakes when  $R_0$  equalled 25 and  $V_C/V_I$  equalled 0.11. These observations were based on some special flow visualisation tests for which the ground was replaced by a glass sheet

smearred with a mixture of titanium dioxide and oil. In fact however, exactly similar conclusions were drawn from the ordinary tests with 3 mm and 6 mm glass beads.

Figure 9 shows that the ingestion boundaries, and therefore the boundaries separating those conditions under which a vortex forms from those which are vortex free, are independent of the Froude number,  $V_I^2/gD$ , (the ratio of the inertial to gravitational forces acting on a particle within the vortex). This confirms that scaling laws concerned only with ingestion boundaries can exclude Froude number from the argument. Thus for a given value of  $V_C/V_I$  and  $(H/D)$ , the thresholds are only dependent on the Rossby number. The results can therefore be replotted in terms of  $V_C/V_I$  against  $R_o$  for various values of  $(H/D)$ . Figure 10 shows such a plot for  $V_C$  at an angle of  $55^\circ$  to the intake centreline which shows, as does Figure 9, that the smaller the Rossby number the more  $V_C/V_I$  has to be increased to prevent ingestion.

Figure 11 shows some effects of the wind direction on the ingestion thresholds. It compares the results that have just been discussed featuring a wind of  $55^\circ$  to the intake axis with further results obtained with a head wind. The differences in intake size can be ignored in the light of the correlation between the results for intakes of different diameters shown in Figure 9. As  $V_C/V_I$  is increased it is seen that at both values of  $(H/D)$  ingestion ceases with the head wind sooner than with the wind blowing across the axis. The difference is appreciable at  $(H/D) = 1.1$  but much less at an  $(H/D) = 1.3$ .

Figure 12 shows how the direction of rotation of the vortex is influenced by the slope of the velocity gradient. No significant difference was observed between ingestion results with gradients of similar magnitudes but of opposite sign.

At this point it should be noted that there is a lower limit to the ingestion zones shown in Figures 9, 10 and 11. That is, a line can be drawn beneath which ingestion, as signified by the movement of the 3 mm and 6 mm beads, no longer occurs. This boundary is shown approximately by the dotted line in Figure 9. The high values of Rossby number associated with this threshold negates any further consideration of this phenomenon as it is outside the ambient conditions thought likely on an airfield.

#### 4.4 Sizes of particle ingested

To further investigate the validity of the laws a series of tests was undertaken to compare the sizes of particle lifted by the two different diameters of model intake when operating under as nearly as possible identical ambient conditions. In fact, because the range of sizes of commercially available glass marbles was limited,  $(H/D)$ ,  $R_o$  and  $V_C/V_I$  were all adjusted experimentally with the 6 in. diameter intake to obtain a condition sufficing to just lift 9 mm glass beads. One particular combination was  $(H/D) = 1.3$ ,  $R_o = 11.0$  and  $V_C/V_I = 0.1$ . The experiment was then repeated with the 12 in. diameter intake with  $(H/D)$  again equal to 1.3. This time however the particle diameter was increased to  $\frac{3}{4}$  in. according to the scaling laws, and the intake velocity also modified according to the laws so as

to maintain a constant Froude number. It was again found that the particles were just lifted from the ground when  $R_0$  and  $V_C/V_I$  equalled 11.0 and 0.09 respectively.

The preceding observations illustrate the limiting strength of the vortex and also the dependence for particle scaling on the Froude number. A further illustration occurred in some isolated tests carried out in connection with a particular engine installation having  $(H/D) = 2.5$ . It was found that even under the most extreme conditions the vortex could barely lift the 6 mm particles from the ground, whereas the 3 mm ones were readily ingested. However these tests were not pursued, for quite apart from the value of  $(H/D)$  lying outside the range of greatest interest, it was also thought with the intake so high above the ground and such a crude apparatus, that there was probably an appreciable variation of  $R_0$  with height.

#### 4.5 Theoretical approximation of vortex formation using potential flow

The experimental flow pattern may be approximated in potential flow by first determining the streamline flow for a rectangular channel, representing the intake, near a wall representing the ground and then considering the position of the stagnation streamline. The addition of only a small amount of circulation to this streamline flow pattern will produce a vortex. A head or tail wind can then be easily superimposed to provide a flow pattern similar to that shown in Figure 13(a), and representative of the actual flow. As the wind is gradually increased the stagnation streamline is blown downwind as in Figure 13(b) and ultimately eliminated. The potential flow picture then resembles that shown in Figure 13(c) so that the stagnation streamline follows exactly the experimentally observed path of the vortex core. For each value of  $(H/D)$  there is therefore a maximum value of  $V_C/V_I$  for which a stagnation streamline and thus the vortex can exist, and these limiting values are plotted in Figure 14. The experimental points plotted in the Figure are taken from the data on which Figures 9 and 11 are based, each point representing an experimental maximum value of  $V_C/V_I$  for ingestion. The points follow exactly the same trend as the theoretical curve but show a limit somewhat short of the theoretical one. This could reflect both the simplifications employed in the theoretical method and perhaps the continued existence of a vortex up to wind speeds rather higher than those corresponding with the cessation of ingestion.

The above treatment, coupled with the premise that the static pressure in the vortex core governs the ingestion limits, leads to an explanation for the influences shown in Figure 10 of  $(H/D)$ ,  $R_0$  and  $V_C/V_I$  on the ingestion process. By developing the simplified treatment outlined above it can be shown that, with all other conditions constant, the static pressure at the foot of the stagnation streamline decreases with  $(H/D)$ . If vorticity is now added to the wind blowing on to the intake then if a vortex is established the pressure around the stagnation streamline foot (the vortex core) is further reduced. This further reduction is substantially independent of  $(H/D)$ , but is a function of  $R_0$ . Thus for a constant value of  $R_0$  the conclusion that the static pressure around the vortex core falls with  $(H/D)$  remains unchanged. It therefore follows that the lower the

(H/D), the greater is the risk of ingestion. If  $R_0$  is decreased, then because of the increased vorticity the static pressure at the vortex core falls and so the risk of ingestion increases.

#### 4.6 Influence of intake diameter

The increasing risk of ingestion as the ratio of (H/D) becomes smaller will be clear from the preceding sections. However it seems possible that the large inlet diameters which in practice tend to be associated with low values of (H/D) may in their own right increase the risk of ingestion. Consider for example two inlets of differing size operating with equal throat velocities in winds featuring identical velocity gradients. Now if in practice the velocity gradient extends for a distance sufficient to span not only the diameter of the smaller inlet, but that of the larger one as well, then because the Rossby number is inversely proportional to inlet diameter it will be smaller for the larger intake. Thus on the evidence of Figures 9, 10 and 11, at a given (H/D),  $V_C/V_I$  will have to be increased to a higher value to blow the vortex away and so eliminate the risk of debris ingestion. This reflects the fact that the velocity differential across the inlet diameter will be greater with the larger intake than with the smaller one, and this will still be so even when both inlets are operating in the same mean approach wind velocity. Thus, whilst the gradients are the same, the circulation with the larger intake will be greater.

#### 5.0 Comparison with other work - and full-scale predictions

The only other quantitative investigation of vortex ingestion known to the author is that of Klein. A first paper<sup>5</sup> published in 1953 described ingestion experiments conducted in quiescent air with a 1 in. diameter inlet connected to an industrial vacuum cleaner. The paper characterised ingested particles by their terminal falling speed, regardless of their physical shape and composition. Thus the experimental data were plotted in the form shown in Figure 15, in which (H/D) appears as a function of the ratio of particle terminal velocity to inlet throat velocity at the threshold of ingestion. A later investigation by Rodert and Garrett<sup>6</sup> with an intake approximately 20 in. throat diameter indicated the role of ambient vorticity in vortex formation and the ability of a head wind of sufficient strength to eliminate the vortex. In 1957 Klein<sup>7</sup> presented data which showed that under certain wind conditions particles much larger than those predicted by the lower sloping line in Figure 15 were ingested; the experimental points plotted with dots in Figure 15 are taken from this Reference.

Confirmation of this observation came from work by Rolls-Royce in 1966 with two different intakes having diameters of 8 in. and 3 ft. The larger intake was tested under gusty atmospheric conditions near the edge of an airfield and gave an ingestion performance noted by the crosses in Figure 15. The present tests with 3 mm and 6 mm particles provide further support, for the ingestion thresholds shown in Figures 9, 10 and 11 can be replotted to extend the original threshold of Klein up to the threshold represented in Figure 15 by the chained line: this it will be seen predicts ingestion over a much wider range of operating conditions than the original line.

The spread of the experimental ingestion thresholds beyond the line first drawn by Klein reflects the widely varying conditions of wind and ambient vorticity at which the observations were made. For particles of a given size and density for example it seems possible to visualise the original line being replaced by a series of parallel lines, each representing a particular ambient condition. However this added complication is not in itself sufficient. Figure 15 suggests that because for a given  $(H/D)$  and ingestion "boundary"  $V_T/V_I$  is uniquely determined, then for a given throat velocity so also is  $V_T$  and thus the particle diameter. Contrary to the evidence of the present experiments therefore, the argument suggests that the maximum diameter of lifted particles is independent of the intake size. The solution to this difficulty requires the addition of further lines to accommodate changes in either particle size or intake diameter. Thus the overall presentation would become extremely complex.

In contrast, the presentation of ingestion thresholds developed by the author aims essentially to define, in quantitative terms, the conditions under which the vortex forms. The resultant Figures 9, 10 and 11 achieve simplicity at the expense of excluding any reference to the size of particles lifted. This omission is not thought important, for the experiments show that whenever the vortex forms there is a risk of debris ingestion. In the light of this it may be unimportant to distinguish between the ingestion of a 2 in. or a 6 in. piece of concrete, for both might be equally damaging. In any case the size of ingested particle is very much a function of ambient vorticity which in practice, although not in controlled laboratory experiments, is thought likely to vary from one instant to the next.

Notwithstanding the preceding remarks, the recent interest in debris ingestion has undoubtedly been fostered to a large degree by predictions that alarmingly large particles can be lifted by the vortex. Such predictions can be readily made on the basis of the scaling laws. Thus for example it was found possible experimentally for glass beads up to 1 in. diameter to be lifted by the vortex formed beneath a 6 in. diameter model intake with  $(H/D)$  equal to one. This would be equivalent to the lifting of 6 in. diameter particles by a 3 ft diameter intake or 12 in. diameter particles by a 6 ft diameter intake at appropriately scaled operating conditions. In the scaling the necessity will be recalled for retaining the same Rossby number at both the model and full-scale, so that the prediction of maximum particle size just made necessarily assumes full-scale Froude and Rossby numbers similar to those employed in the model work. Confidence that these might not be too significantly different is encouraged by the broad agreement shown in Figure 15 between the chained line representing the extremity of the ingestion prone area on the plot, as determined by 3 mm particles with the 6 in. intake, and the points obtained by Rolls-Royce under gusty airfield conditions with a 3 ft diameter intake.

## 6.0 The prevention of ingestion

Although this Report is concerned with the mechanics of the ingestion process, the author has devoted some time studying methods by which ingestion might be avoided. Numerous possibilities have been examined experimentally. These have comprised aerodynamic devices such as the blowing jet

extensively used in earlier investigations<sup>7,8</sup> and mechanical arrangements such as plates which physically impede the progress of any lifted particle. Some undoubtedly reduced the frequency of ingestion, but at the low values of  $(H/D)$  currently of greatest interest, none provided an absolute safeguard.

Against this background it is suggested that a promising operational technique might be to keep the ratio of  $V_C/V_I$  as high as possible, for it will be seen from Figure 14 that if the ratio can be kept sufficiently high the vortex will not form at all. From this point of view the worst thing is to run an engine up to full speed under quiescent conditions, for in this way  $V_I$  reaches a maximum whilst  $V_C$  remains effectively zero.  $V_C/V_I$  is thus effectively zero, and local disturbances would almost certainly preclude the reproduction of the laboratory condition featuring freedom from vortex formation. Keeping  $V_C/V_I$  as high as possible during the very early phase of take-off demands a progressive throttle opening as the aircraft accelerates, so that  $V_C$  increases with  $V_I$ . It is also worth noting that so far as the impulsive projection of particles by the vortex is concerned, the ingestion problem may be eased by the aircraft movement, for this might tend to cause particles to strike the underside of the intake cowling.

## 7.0 Conclusions

The ingestion of debris during ground running by the low slung intakes featured in current aircraft projects can occur through two mechanisms associated with the formation of a vortex beneath the intake. Particles on the ground near the vortex extremities tend to be blown horizontally, and those that bounce can become airborne under the influence of the local air currents. Dramatically different in the manner of lifting is the action of the vortex on those particles over which the vortex core passes, for with a vortex of sufficient strength these particles are projected violently upwards, as if under the action of an impulsive force.

Scaling laws have been developed to relate model and full-scale tests of the lifting of particles by the vortex core. The laws are:

- (1) Particle size is proportional to test scale.
- (2) Intake velocity squared is proportional to test scale.
- (3) Ratio of particle density to fluid density is the same for both full-scale and model tests. Thus for tests at both scales in air the particle densities should be the same.
- (4) Ratio of cross wind velocity to intake throat velocity is the same for model and full-scale tests.
- (5) Ratio of the intake velocity to the product (cross wind velocity gradient  $\times$  intake diameter) is the same for model and full size tests.

Experimental results support the validity of these laws and suggest for example, that a 6 ft diameter intake operating with its centreline 6 ft above the ground could give rise to a vortex capable of lifting spherical concrete blocks 1 ft in diameter. Various methods of reducing ingestion

were examined experimentally and although some undoubtedly decreased the frequency of ingestion, none provided an absolute safeguard. However, an operational technique which might ease the ingestion problem involves a progressive throttle opening as the aircraft initially accelerates on take-off so as to keep as high as possible the ratio of the wind velocity blowing on to the intake to the intake velocity.



REFERENCES

<u>No.</u>	<u>Author(s)</u>	<u>Title, etc.</u>
1	M. Cox	The scaling of experiments involving particle entrainment and recirculation Unpublished work at N.G.T.E. August 1963
2		Scaling laws for model tests on intake debris ingestion Unpublished work at Rolls-Royce (Hucknall) July 1966
3	B. R. Morton	Geophysical Vortices, Progress in Aeronautical Sciences, Vol. 7, Ed. D. Kuchemann Publisher Pergamon Press Ltd., 1966
4	J. F. Norbury	Some observations of vortices formed at a duct entry near a plane surface Lecture presented at Symposium on Concentrated Vortex Motions in Fluids - Ann Arbor Michigan, 1964
5	H. Klein	Small scale tests on jet engine pebble aspiration Douglas Aircraft Co. Report No. SM.14895 August 1953
6	L. A. Rodert F. B. Garret	Ingestion of foreign objects into turbine engines by vortices N.A.C.A., TN.3330, February 1955
7	H. Klein	An aerodynamic screen for jet engines I.A.S. Preprint No. 676 on Douglas Aircraft Co., Report No. SM.22625 January 1957
8	G. T. Golesworthy	Tests of a blow-away jet debris guard applied to a supersonic turbo-jet intake A.R.C. CP. No. 561, 1959
9	Z. M. Jawor	Unpublished work at N.G.T.E. December 1966
10	L. Prandtl O. G. Tietjens	Fundamentals of hydro- and aero-mechanics Publisher McGraw-Hill Book Co. Ltd. 1934

APPENDIX I

List of symbols

C	velocity of sound
D	intake diameter
d	particle diameter
F	force
f	functions
g	gravitational constant
H	intake height
L	length
K	constants
p	pressure
r	radius associated with vortex
V	velocity
w	velocity gradient
$\delta$	boundary layer thickness
$\rho$	density
$\theta$	direction of cross wind with respect to the intake centreline
$\tau$	circulation
$\mu$	viscosity
$\omega$	angular velocity
$C_D$	drag coefficient
$F_r$	Froude number
$M_n$	Mach number
$R_e$	Reynolds number
$R_o$	Rossby number = $\frac{V_I}{wD}$

APPENDIX I (cont'd)

Subscripts

a	air
C,c	cross wind
I	intake
F.S.	full-scale
p	particle
i	interface of inner and outer regions of vortex
M	model scale
r	radius
T	terminal (velocity)

APPENDIX II

Dimensional analysis of particle lifting by ground vortex

Using the notation of Appendix I, and following the conventional pattern of dimensional analysis the variables associated with the lifting of a particle are noted and listed as follows. See also Figure 1.

$$V_I, V_C, \rho_a, \rho_p, \mu_a, C_a, D, H, \delta, d, g, F, w_c$$

From the 13 variables listed above 3 prime variables may be chosen to represent the 3 prime concepts of mass, length and time.

For this analysis the prime variables may be chosen as follows.

- (i) D intake diameter - geometric similarity.
- (ii)  $V_I$  intake velocity - kinematic similarity.
- (iii)  $\rho_a$  density of air - dynamic similarity.

The remaining 10 variables must be arranged into groups and balanced dimensionally with respect to the prime variables.

The 10 groups can be expressed as follows.

$$\frac{V_C}{(\rho_a^{\alpha_1} V_I^{\alpha_2} D^{\alpha_3})}, \frac{\mu_a}{(\rho_a V_I D)^\beta}, \frac{C_a}{(\rho_a V_I D)^\gamma}, \frac{d}{(\rho_a V_I D)^\delta}, \frac{\rho_p}{(\rho_a V_I D)^\epsilon},$$

$$\frac{g}{(\rho_a V_I D)^\kappa}, \frac{H}{(\rho_a V_I D)^\sigma}, \frac{\delta}{(\rho_a V_I D)^\omega}, \frac{F}{(\rho_a V_I D)^\xi}, \frac{w_c}{(\rho_a V_I D)^\tau}$$

in which for brevity, the second group  $\frac{\mu_a}{\rho_a^{\beta_1} V_I^{\beta_2} D^{\beta_3}}$  has been written

$$\frac{\mu_a}{(\rho_a V_I D)^\beta} \text{ and similarly in the remaining groups.}$$

Substituting the dimensions of the variables in group 1

$$\frac{V_C}{\rho_a^{\alpha_1} V_I^{\alpha_2} D^{\alpha_3}} = \frac{L T^{-1}}{(ML^{-3})^{\alpha_1} (LT^{-1})^{\alpha_2} (L)^{\alpha_3}}$$

and equating the indices yields

$$1 = 3a_1 + a_2 + a_3 \quad - \text{ length}$$

$$-1 = -a_2 \quad - \text{ time}$$

$$0 = a_1 \quad - \text{ mass}$$

$$\therefore a_1 = 0 \quad a_2 = 1 \quad a_3 = 0$$

Hence the non-dimensional form of group 1 becomes  $\frac{V_C}{V_I}$ . Similar relationships may be found for the other 9 groups; the results of which are given below

$$\begin{array}{ccccccc} \frac{V_C}{V_I}, & \frac{\mu_a}{\rho_a V_I D}, & \frac{C_a}{V_I}, & \frac{d}{D}, & \frac{\rho_p}{\rho_a}, & \frac{gD}{V_I^2}, & \frac{H}{D}, \frac{\delta}{D}, \frac{F}{\rho_a V_I^2 D^2}, \frac{w_c D}{V_I}. \\ | & | & | & | & | & | & | \\ \text{Reynolds} & \text{Mach} & & & \text{Froude} & & \text{Rossby} \\ \text{number} & \text{number} & & & \text{number} & & \text{number} \end{array}$$

Therefore the force acting on a particle can be expressed by

$$\frac{F}{\rho_a V_I^2 D^2} = f \left( \frac{V_C}{V_I}, \frac{\mu_a}{\rho_a D V_I}, \frac{C_a}{V_I}, \frac{d}{D}, \frac{\rho_p}{\rho_a}, \frac{gD}{V_I^2}, \frac{H}{D}, \frac{\delta}{D}, \frac{w_c D}{V_I} \right)$$

For complete similarity between full-scale and model tests each of the dimensionless groups should be identical at both scales. However this would entail the model tests being carried out in a pressurised chamber in order to achieve, for example, full-scale Reynolds numbers in the model experiment. In fact, however, model tests are clearly most readily performed under atmospheric conditions. In these circumstances the only non-dimensional groups in which equality can be maintained between full-scale and model are as follows:-

$$\frac{V_C}{V_I}, \frac{\rho_p}{\rho_a}, \frac{H}{D}, \frac{d}{D}, \frac{w_c D}{V_I}$$

Thus it is necessary to investigate the magnitude of the effects of the remaining non-dimensional groups on the ingestion process. In this respect a review of earlier work is helpful. Although previous studies<sup>5 to 9</sup> of what is undoubtedly a complex phenomenon fall far from completely explaining the processes involved, it is nevertheless not unreasonable to draw the following conclusions:-

- (a) The vortex tends to wander, and any particle on the ground in the path of the vortex core is subject to an impulsive force which if sufficiently strong relative to the forces resisting motion will lift the particle. The particle is projected impulsively into the air, and under these conditions viscous effects barely influence the initial trajectory.
- (b) Only particles constrained and subject to the stagnation region of the inlet vortex are picked up. Thus the effects of Mach number on the stagnation streamline may be ignored as the non-dimensional flow field is independent of Mach number.

The only remaining parameter is the Froude number. Thus an approximate expression for the force acting on a particle may be defined as follows

$$F = \rho_a V_I^2 D^3 f \left( \frac{V_C}{V_I}, \frac{d}{D}, \frac{\rho_p}{\rho_a}, \frac{gD}{V_I^2}, \frac{H}{D}, \frac{w_c D}{V_I} \right)$$

In an experimental investigation concerned both with determining the size of particle that can be lifted, as well as the ingestion thresholds separating the conditions under which vortex ingestion can occur from those which are ingestion free, the above expression leads to the requirement for observing the following scaling laws to achieve similarity between full-scale ingestion and model experiments.

- (1) Particle size is proportional to test scale.
- (2) Intake velocity squared is proportional to test scale.
- (3) Ratio of particle density to fluid density is the same for both full-scale and model tests. Thus for tests at both scales in air the particle densities should be the same.
- (4) Ratio of cross wind velocity to intake velocity is the same for model and full size tests.
- (5) Ratio of the intake velocity to the product (cross wind velocity gradient  $\times$  intake diameter) is the same for model and full size tests. This is equivalent to the Rossby number as noted in the body of the Report.

APPENDIX III

Analysis of particle lifting based on the pressure distribution within a simple vortex

The rules for scaling model and full-scale tests may also be deduced by resolving the forces acting on a particle within the field of influence of a simplified vortex. Consider a vortex with a core of constant angular rotation,  $\omega$ , and an outer region of nominally free vortex flow in which  $\omega r^2 = \text{constant}$ , as for example in Reference 10. The corresponding pressure distribution can be calculated using the radial equilibrium equation as follows:-

In circular motion the pressure increases radially outwards and thus for radial equilibrium

$$\frac{1}{\rho} \frac{dp}{dr} = \frac{V^2}{r} \quad \dots(\text{III.1})$$

If the pressure at infinity is  $p_a$  then for any finite point at radius  $r$  the pressure is

$$p = p_a - \int_r^{\infty} \frac{\rho V^2}{r} dr \quad \dots(\text{III.2})$$

If the density variations are ignored i.e.,  $\rho = \rho_a$ , then the pressure distribution may be calculated for the inner core and outer region.

(a) Outer region

This is defined in Figure 16, as the region in which

$$r_1 < r < \infty.$$

Now in the outer region,

$$V = \frac{\tau}{2\pi r} \quad \dots(\text{III.3})$$

Whence, evaluating the integral of Equation (III.2)

$$\rho_a \int_r^\infty \frac{V^2}{r} dr = \frac{\rho_a \tau^2}{4\pi^2} \int_r^\infty \frac{dr}{r^3} = \frac{\rho_a \tau^2}{8\pi^2 r^2} \dots(III.4)$$

So that from Equation (III.2)

$$p = p_a - \frac{\rho_a \tau^2}{8\pi^2 r^2} \dots(III.5)$$

Therefore the pressure at the interface radius  $r_i$  is

$$p_i = p_a - \frac{\rho_a \tau^2}{8\pi^2 r_i^2} \dots(III.6)$$

(b) Inner region

Referring again to Figure 16, it will be seen that in this region

$$0 < r < r_i$$

Also in the inner region

$$V = \frac{v_r}{2\pi r_i} \dots(III.7)$$

Evaluating the integral of Equation (III.2) once again

$$\rho_a \int_r^{r_i} \frac{V^2}{r} dr = \frac{\rho_a \tau^2}{4\pi^2 r_i^2} \int_r^{r_i} r dr = \frac{\rho_a \tau^2}{8\pi^2 r_i^2} (r_i^2 - r^2) \dots(III.8)$$



So that, the pressure at radius r is given by

$$p = p_i - \frac{\rho_a \tau^2}{8\pi^2 r_i^4} (r_i^2 - r^2) \quad \dots(III.9)$$

where  $p_i$  is given by Equation (III.6).

Determination of lifting forces acting on particle

The pressure distributions derived above for the inner and outer regions can now be used to calculate the forces acting on a particle of radius  $r_p$  centrally situated at the foot of the vortex. Two cases are considered. In the first the particle diameter is greater than that of the core, i.e.,  $r_p > r_i$ . In the second,  $r_p < r_i$ .

(a) Particle diameter greater than the vortex core,  $r_p > r_i$

The force on the particle due to vortex alone may be determined by the summation of pressure distribution on the particle.

$$\text{FORCE, } F = \int_0^{r_p} p 2\pi r dr \quad \dots(III.10)$$

and substituting for p from Equations (III.5), (III.6) and (III.9) gives

$$F = \int_0^{r_i} \left( p_a - \frac{\rho_a \tau^2}{4\pi^2 r_i^2} + \frac{\rho_a \tau^2 r^2}{8\pi^2 r_i^4} \right) 2\pi r dr + \int_{r_i}^{r_p} \left( p_a - \frac{\rho_a \tau^2}{8\pi^2 r^2} \right) 2\pi r dr \quad \dots(III.11)$$

$$= p_a \pi r_i^2 - \frac{\rho_a \tau^2 \pi r_i^2}{4\pi^2 r_i^2} + \frac{\rho_a \tau^2 r_i^4 \pi}{16\pi^2 r_i^4} + p_a \pi (r_p^2 - r_i^2) - \frac{\rho_a \tau^2 \pi \ln \left( \frac{r_p}{r_i} \right)}{4\pi^2} \quad \dots(III.12)$$

$$= p_a \pi r_p^2 - \frac{3}{16} \frac{\rho_a \tau^2}{\pi} - \frac{\rho_a \tau^2 \ln \left( \frac{r_p}{r_i} \right)}{4\pi} \quad \dots(III.13)$$

When the particle is on the point of being lifted by the vortex the following equality holds:-

FORCE ON LOWER SURFACE OF PARTICLE DUE TO AMBIENT CONDITIONS - FORCE ON  
UPPER SURFACE OF PARTICLE DUE TO VORTEX = WEIGHT OF PARTICLE

.....(III.14a)

$$\text{i.e.,} \quad p_a \pi r_p^2 - F = \frac{4}{3} \pi r_p^3 \rho_p g \quad \text{.....(III.14b)}$$

From which it follows that, using Equation (III.13)

$$\frac{\rho_p g r_p}{\rho_a v_{r_p}^2} = \frac{3}{4} \left( \frac{3}{4} + \ln \frac{r_p}{r_1} \right) \quad \text{.....(III.15a)}$$

$$\text{But} \quad v_{r_p}^2 = \omega_p^2 r_p^2$$

$$\therefore \quad \frac{\rho_p g r_p}{\rho_a \omega_p^2 r_p^2} = \frac{3}{4} \left( \frac{3}{4} + \ln \frac{r_p}{r_1} \right) \quad \text{.....(III.15b)}$$

(b) Particle diameter less than the vortex core  $r_p < r_1$

As before, the force due to the vortex on the particle is derived by summing the pressures acting on the particle.

$$\text{Thus,} \quad \text{FORCE, } F = \int_0^{r_p} p 2\pi r dr \quad \text{.....(III.16)}$$

and substituting for p from Equations (III.6) and (III.9) gives

$$F = \int_0^{r_p} \left( p_a - \frac{\rho_a \tau^2}{4\pi^2 r_i^2} + \frac{\rho_a \tau^2 r^2}{8\pi^2 r_i^4} \right) 2\pi r dr \quad \dots(III.17)$$

$$= p_a \pi r_p^2 - \frac{\rho_a \tau^2 \pi r_p^2}{4\pi^2 r_i^2} + \frac{\pi \rho_a \tau^2 r_p^4}{16\pi^2 r_i^4} \quad \dots(III.18)$$

Equating verticle forces on the particle as in Equation (III.14a and b)

$$\frac{\rho_p g r_p}{\rho_a v_{r_p}^2} = \frac{3}{4} \left( 1 - \frac{r_p^2}{4r_i^2} \right) \frac{r_i^2}{r_p^2} \quad \dots(III.19a)$$

But  $v_{r_p}^2 = \omega_p^2 r_p^2$

$$\frac{\rho_p g r_p}{\rho_a \omega_p^2 r_p^2} = \frac{3}{4} \left( 1 - \frac{r_p^2}{4r_i^2} \right) \frac{r_i^2}{r_p^2} \quad \dots(III.19b)$$

Derivation of scaling laws

For equivalence between model and full-scale tests the following conditions must hold.

- (a) For the case when  $r_p > r_i$

$$\frac{\left( \frac{\rho_p \xi r_p}{\rho_a \omega_p^2 r_p^2} \right)_{F.S.}}{\left( \frac{\rho_p \xi r_p}{\rho_a \omega_p^2 r_p^2} \right)_M} = \frac{\left[ \frac{3}{4} \left( \frac{3}{4} + \ln \frac{r_p}{r_i} \right) \right]_{F.S.}}{\left[ \frac{3}{4} \left( \frac{3}{4} + \ln \frac{r_p}{r_i} \right) \right]_M} \dots(III.20)$$

(b) For the case when  $r_p < r_i$

$$\frac{\left( \frac{\rho_p \xi r_p}{\rho_a \omega_p^2 r_p^2} \right)_{F.S.}}{\left( \frac{\rho_p \xi r_p}{\rho_a \omega_p^2 r_p^2} \right)_M} = \frac{\left[ \frac{3}{4} \frac{r_i^2}{r_p^2} \left( 1 - \frac{r_p^2}{4r_i^2} \right) \right]_{F.S.}}{\left[ \frac{3}{4} \frac{r_i^2}{r_p^2} \left( 1 - \frac{r_p^2}{4r_i^2} \right) \right]_M} \dots(III.21)$$

Now if the model is scaled linearly with respect to the full size intake and the cross wind velocity gradient,  $w_c$ , is assumed to be proportional to the vortex angular velocity,  $\omega$ , i.e.,

$$\left( \frac{r_i}{r_p} \right)_{F.S.} = \left( \frac{r_i}{r_p} \right)_M \dots(a)$$

$$\left( \frac{r_p}{D} \right)_{F.S.} = \left( \frac{r_p}{D} \right)_M \dots(b)$$

where D is intake diameter,

$$\text{and} \quad \omega_p r_p = f_1 (w_c r_p) = f_2 (V_C) \dots(c) \quad \dots(III.22)$$





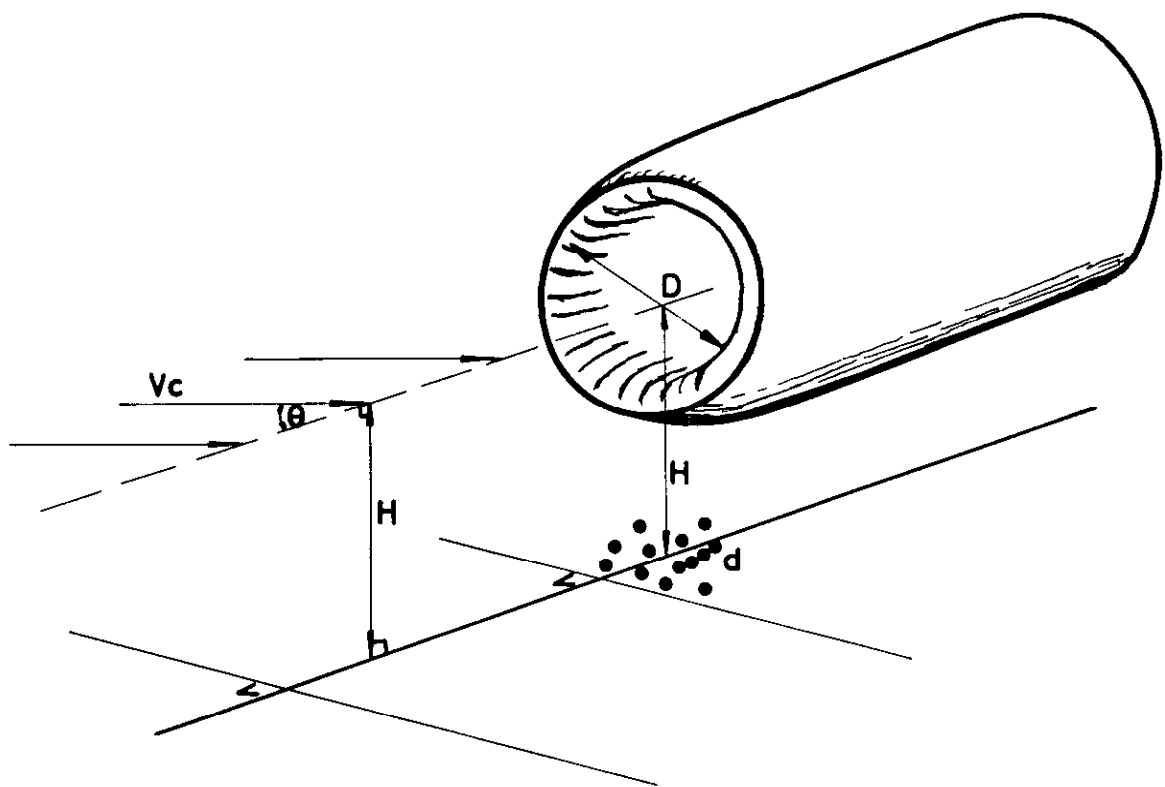


FIG.1 GENERAL ARRANGEMENT AND NOMENCLATURE  
FOR INTAKE

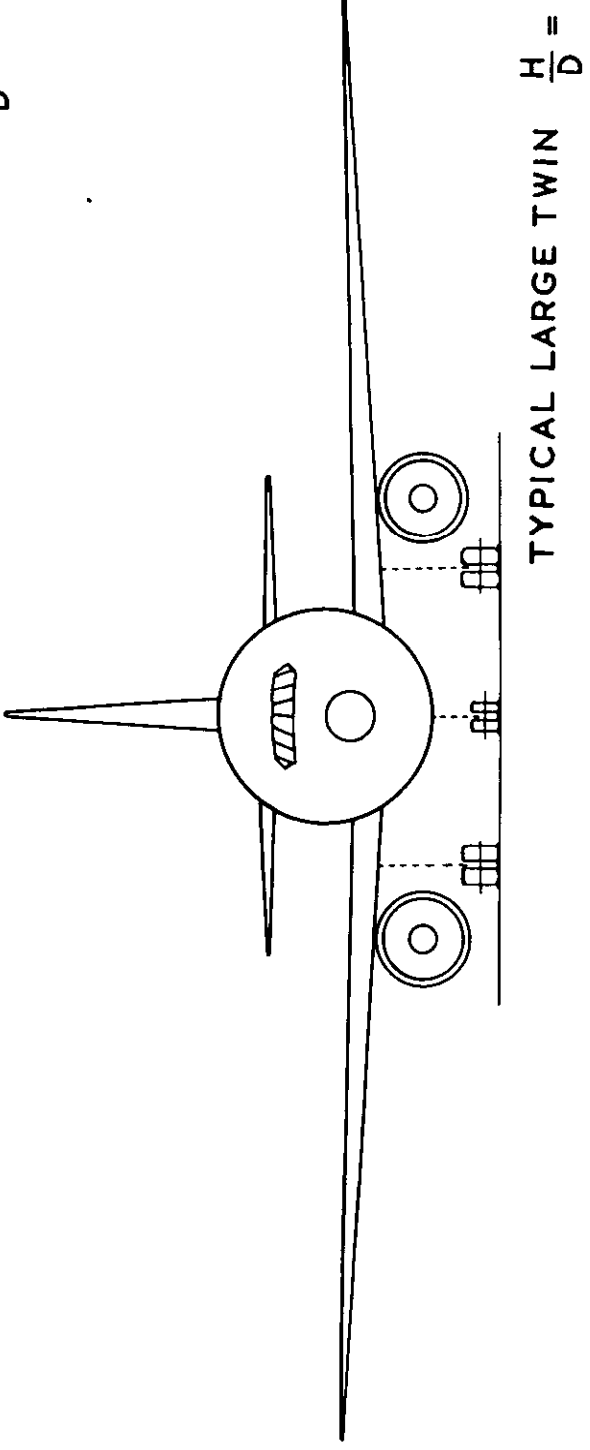
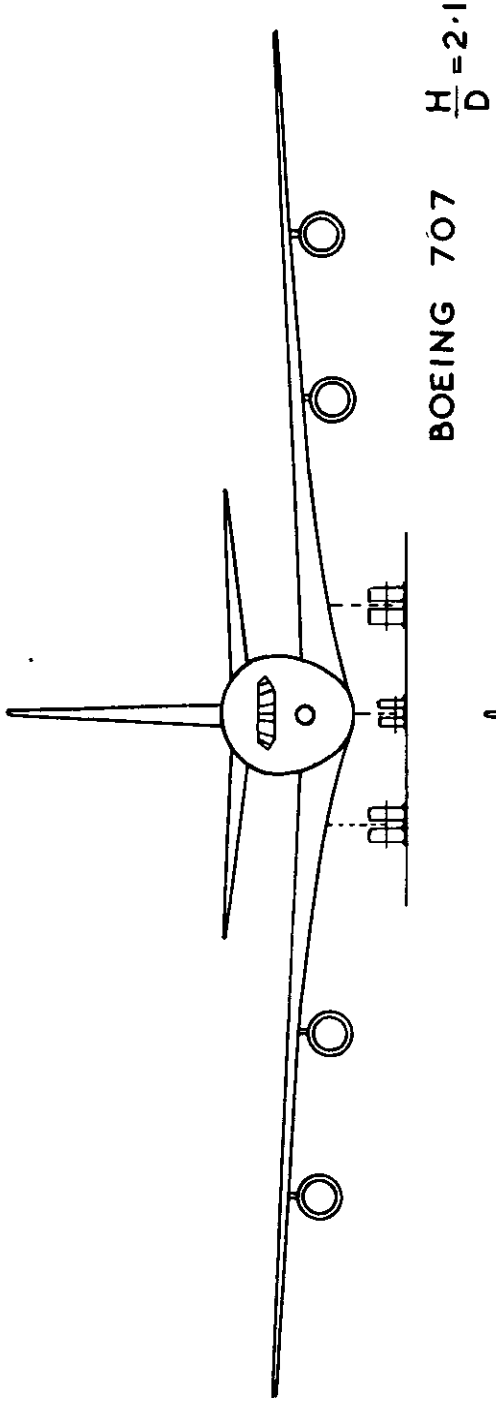


FIG.2 COMPARISON BETWEEN CURRENT AND POSSIBLE TRANSPORTS IN TERMS OF H/D RATIO



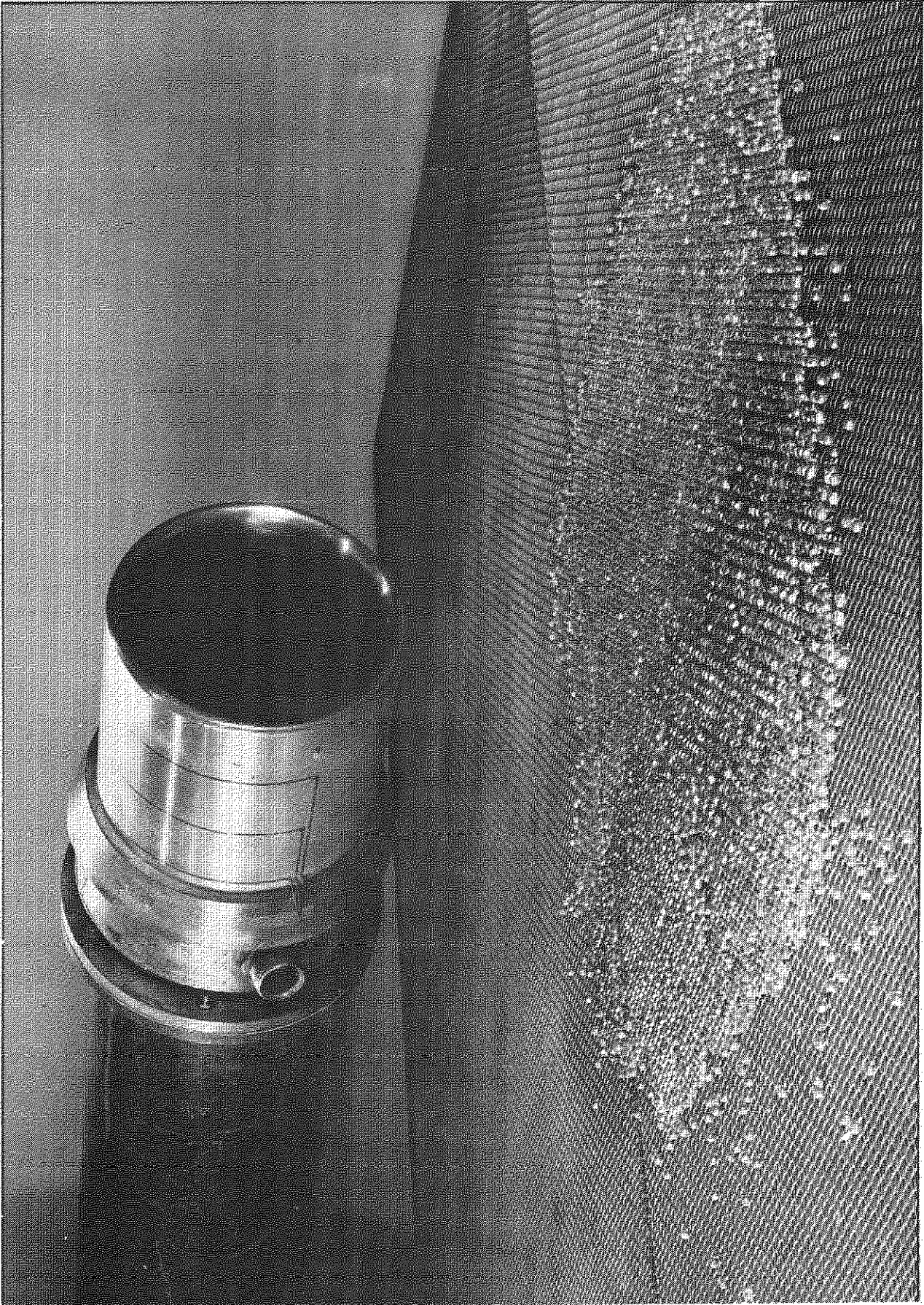


FIG 3. PARTICLE INGESTION RIG SHOWING 6in. DIAMETER INTAKE  
( $H/D=1.4$ , GROUND DEBRIS SIMULATED BY 6mm GLASS BEADS).

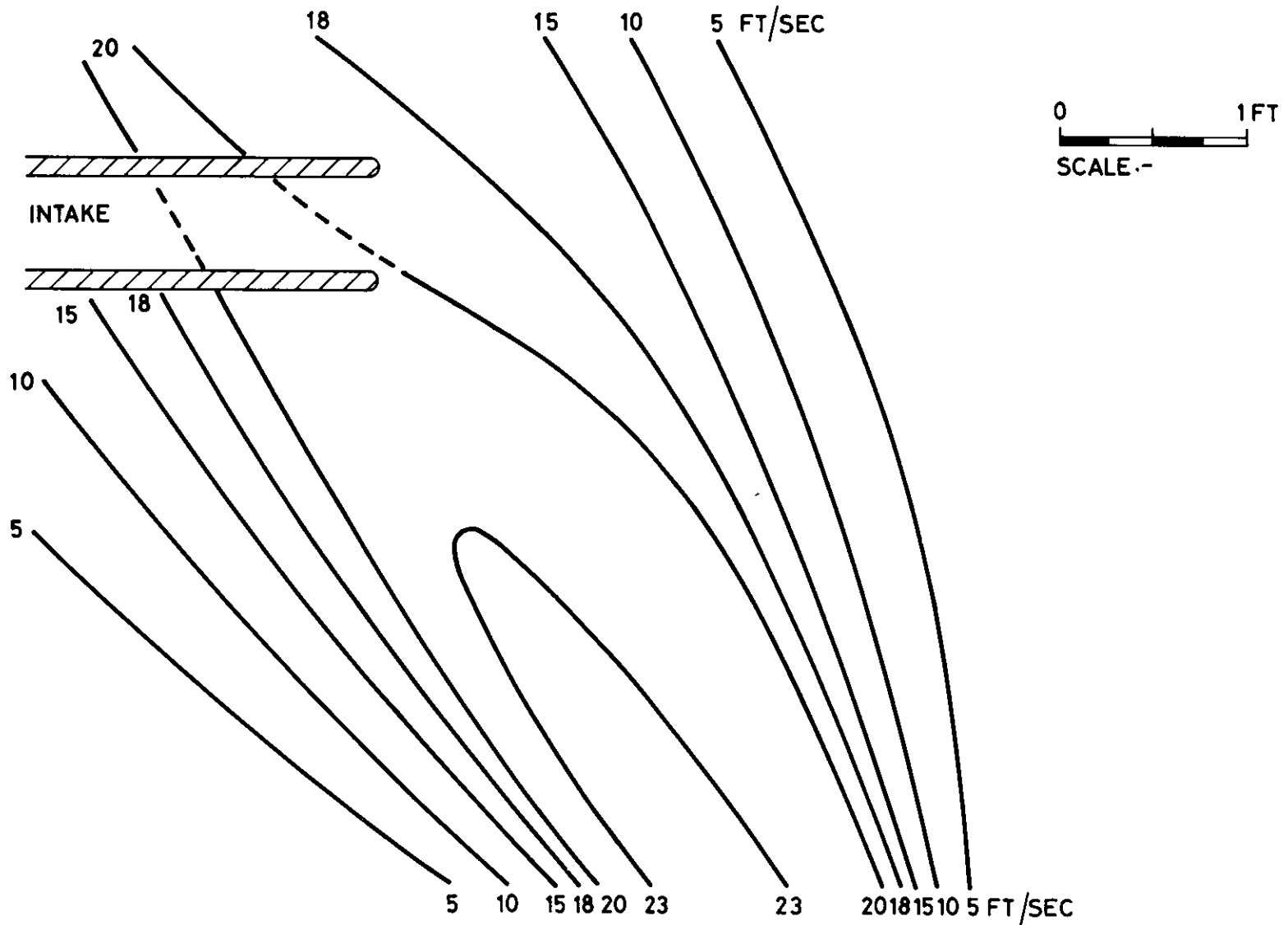


FIG.4 TYPICAL VELOCITY PROFILE IN PLANE PARALLEL TO THE GROUND :  
 $V_c$  AT AN ANGLE OF  $55^\circ$  TO INTAKE  $\zeta$

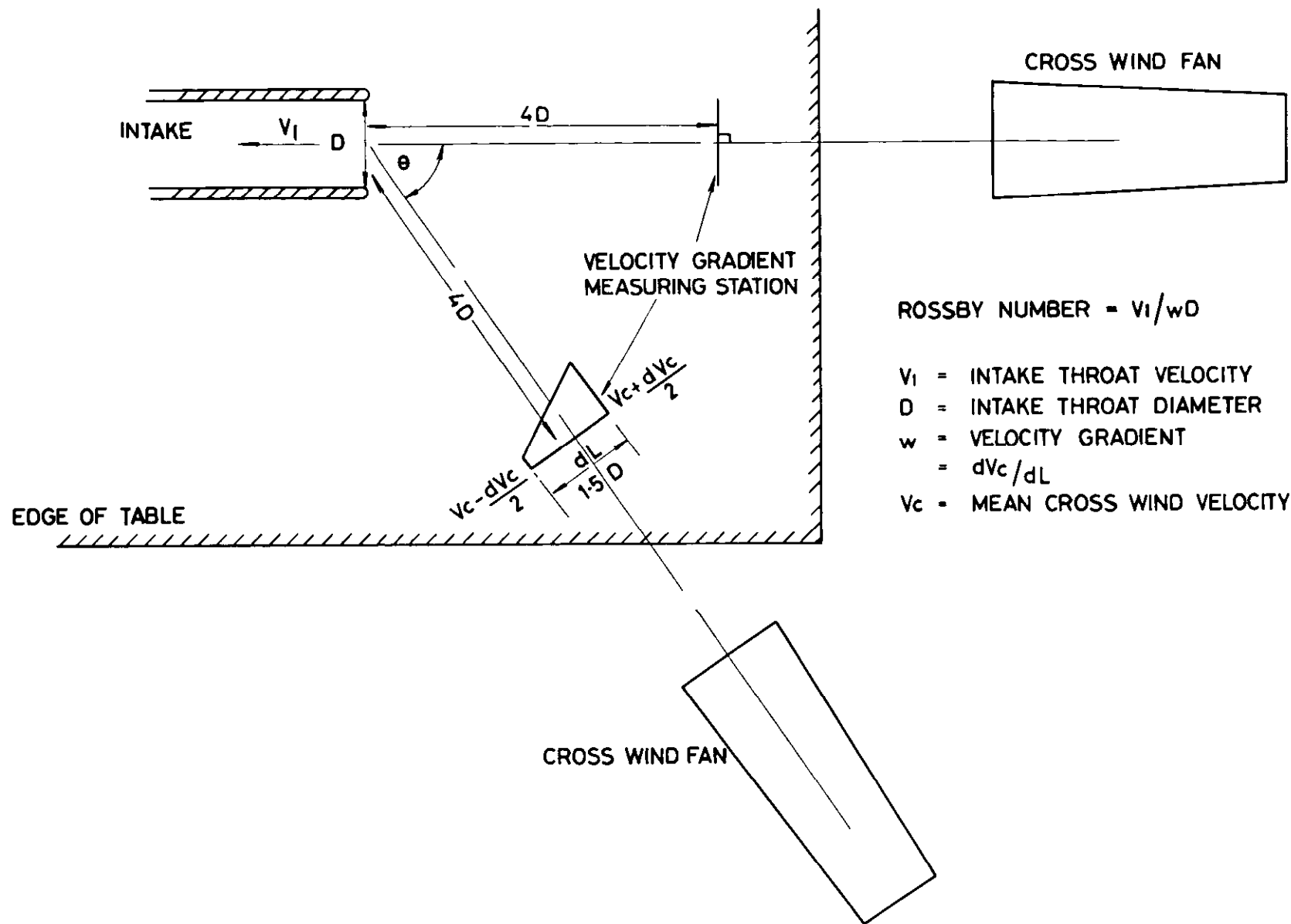


FIG.5 PLAN VIEW OF INTAKE INGESTION RIG SHOWING STATIONS FOR MEASURING VELOCITY PROFILES



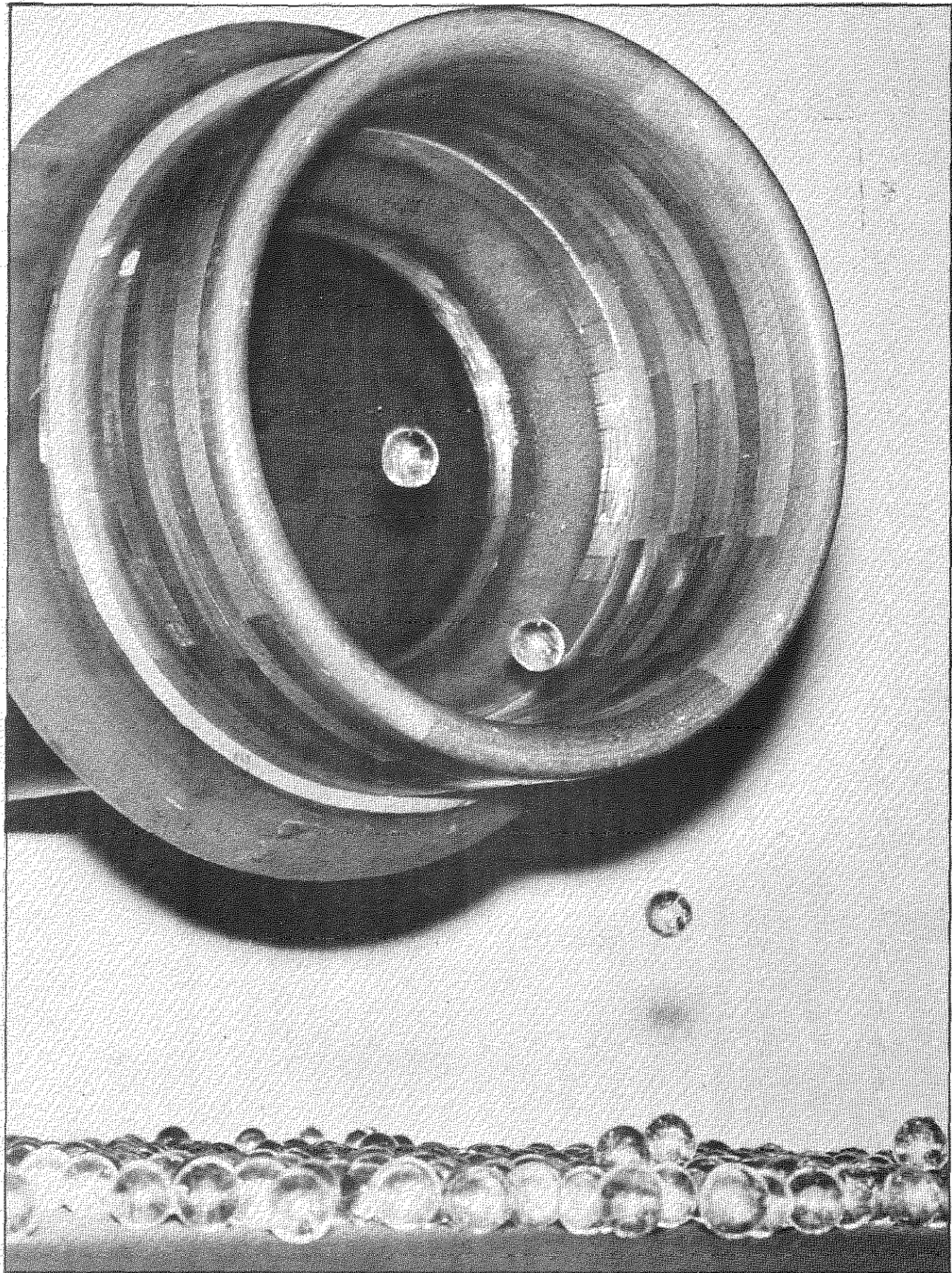
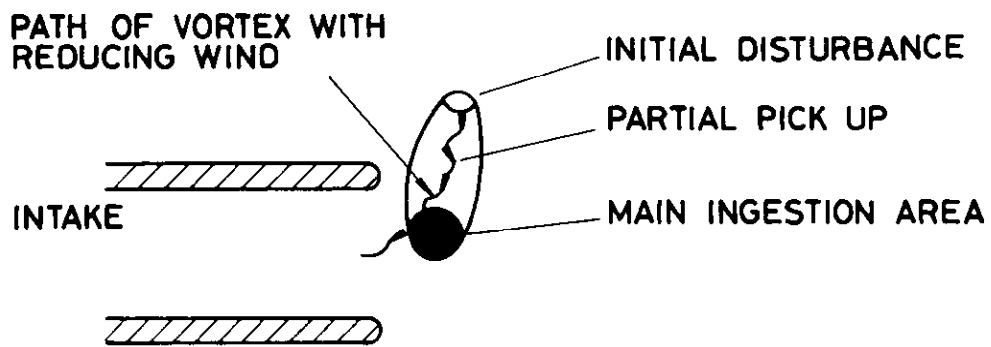
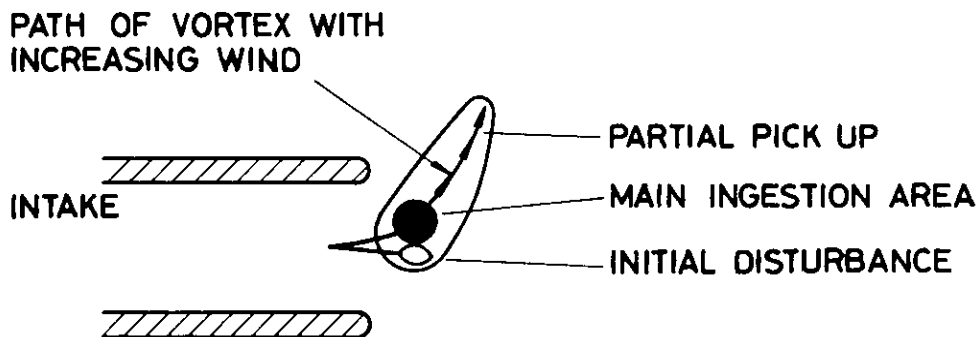


FIG.6 12in DIAMETER INTAKE AT AN  $H/D=1.2$   
SHOWING INGESTION OF 1in. DIAMETER GLASS BALLS.



$V_c$  DECREASING



$V_c$  INCREASING

FIG.7 GENERAL PATTERN OF INGESTION FOR VARYING CROSS WINDS

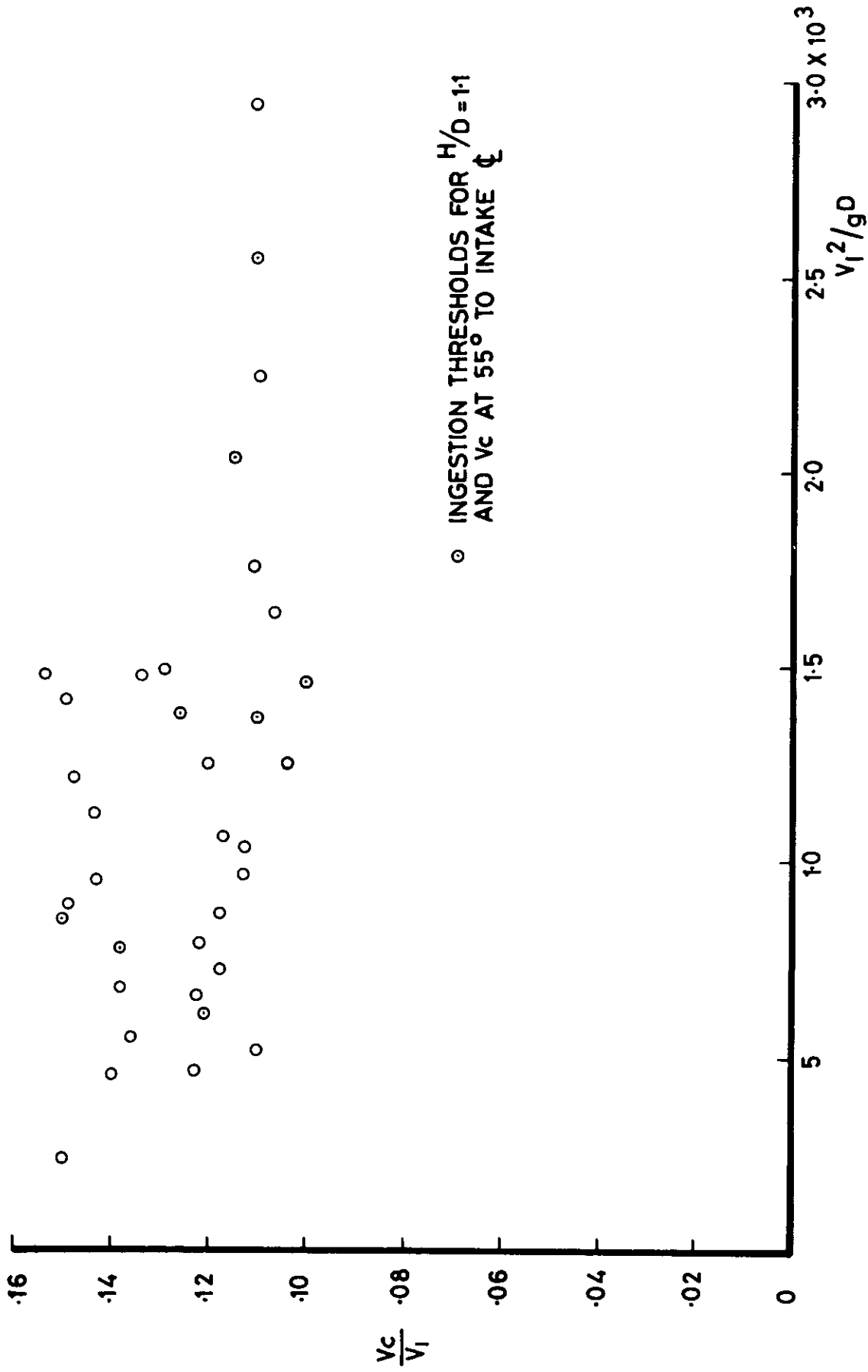


**FIG.8 SAMPLE EXPERIMENTAL RESULTS**

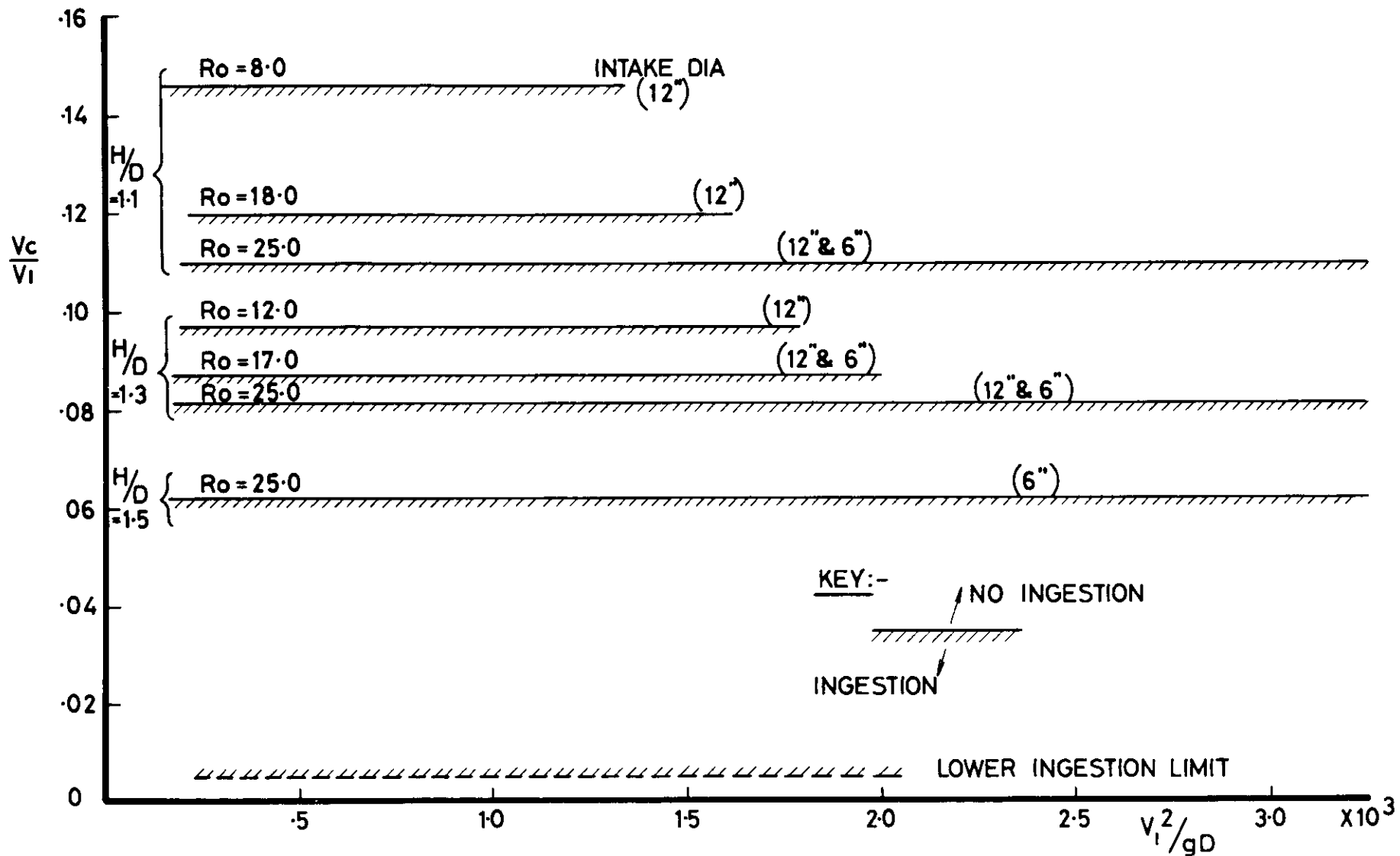


FIG.9 INGESTION BOUNDARIES IN TERMS OF  $\frac{V_c}{V_i}$  AND  $\frac{V_i^2}{gD}$

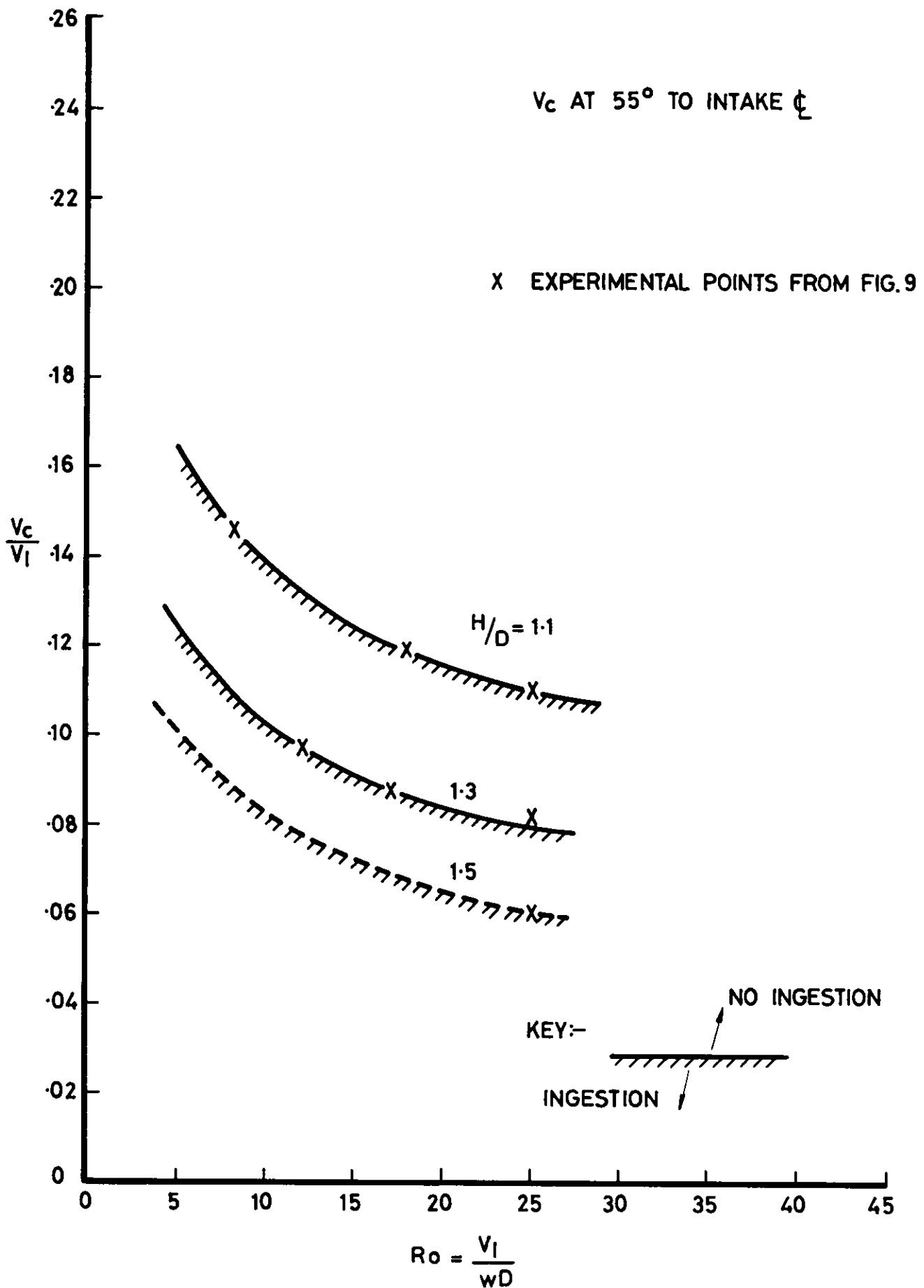


FIG.10 INGESTION BOUNDARIES IN TERMS OF  
 $\frac{V_c}{V_1}$  AND  $\frac{V_1}{wD}$



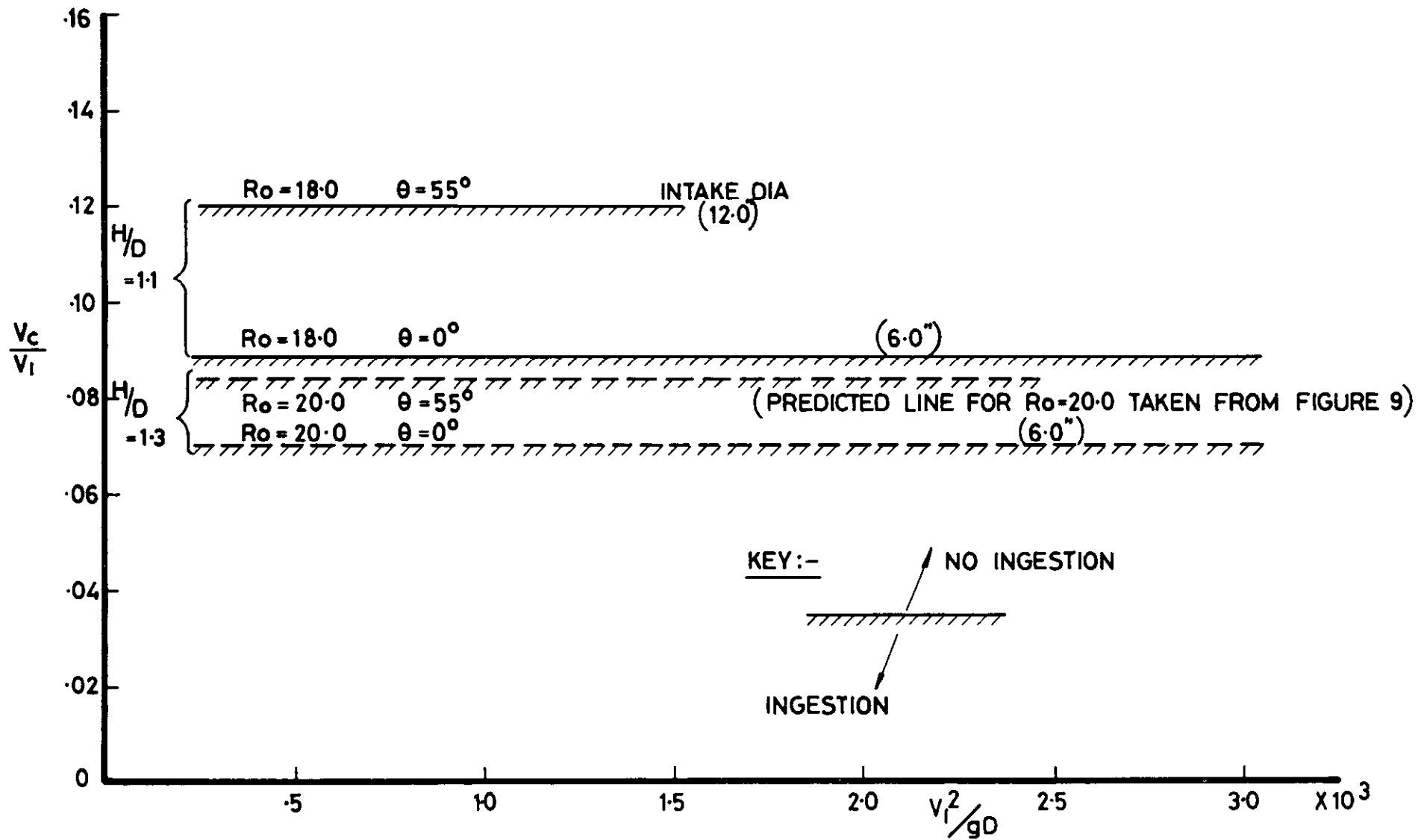
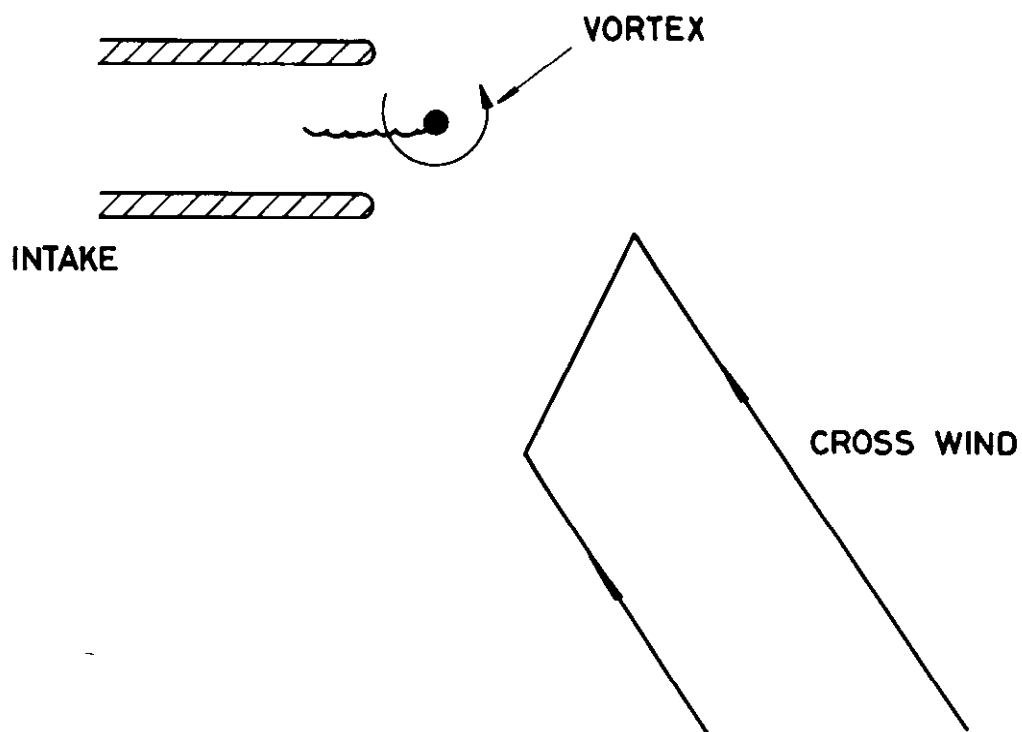


FIG.11 VARIATION OF INGESTION BOUNDARIES WITH RESPECT TO CROSS WIND DIRECTION



PLAN VIEWS LOOKING DOWN ON TO THE GROUND

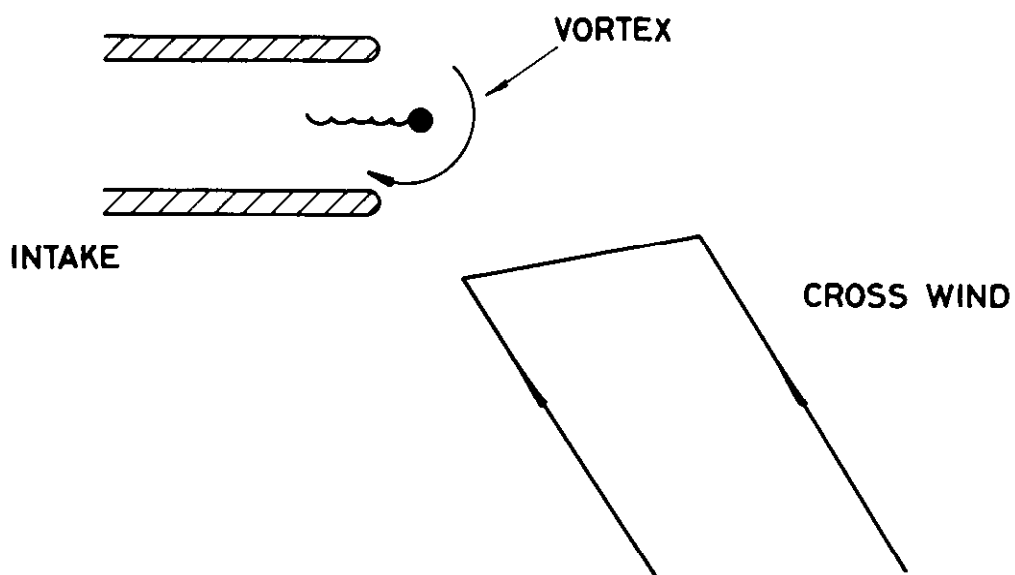
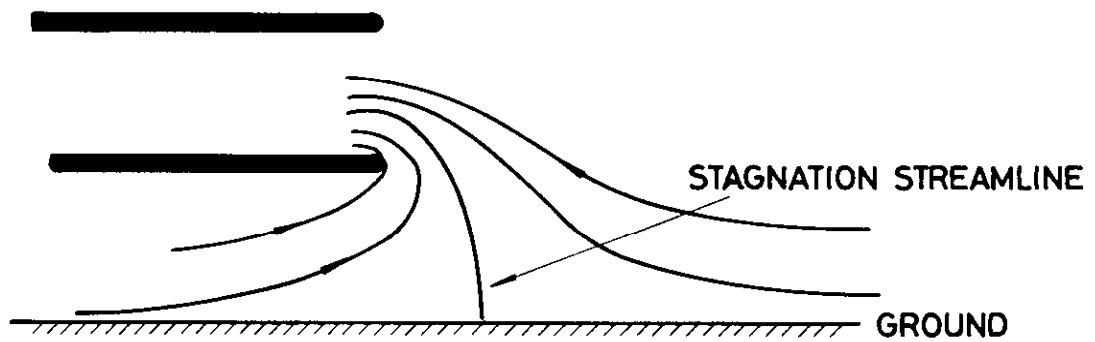


FIG.12 DIRECTION OF ROTATION OF VORTEX WITH RESPECT TO CROSS WIND GRADIENT

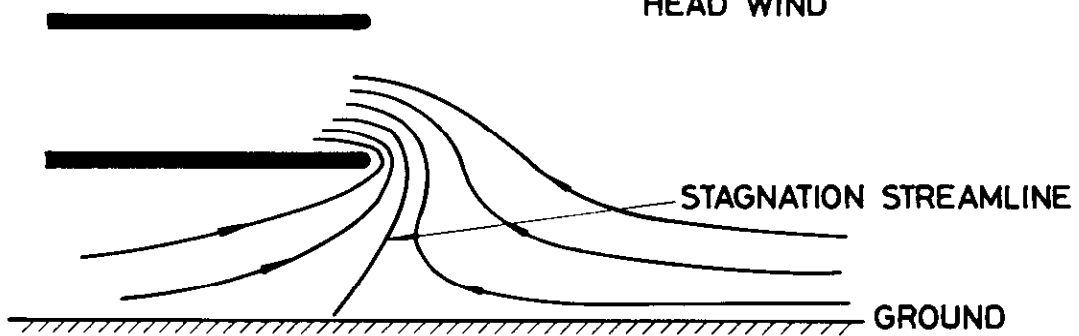
(a)

ZERO HEAD WIND



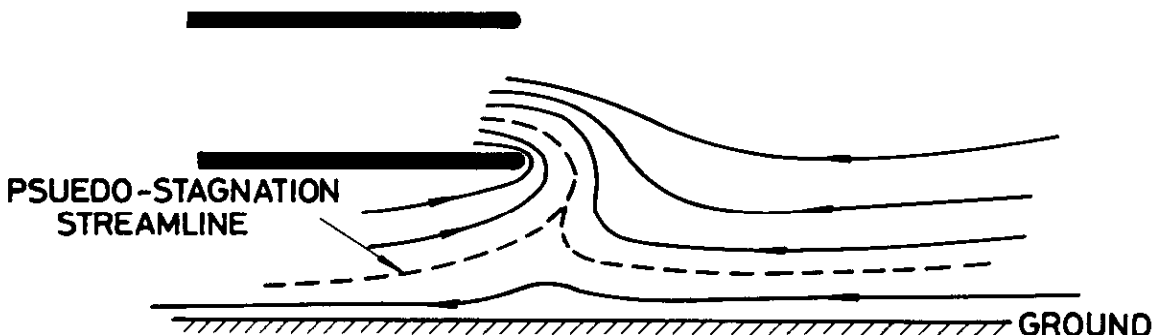
(b)

HEAD WIND



(c)

HEAD WIND



FIGS.13 a b & c EFFECT OF VARYING HEAD WIND ON INTAKE STREAMLINE FLOW

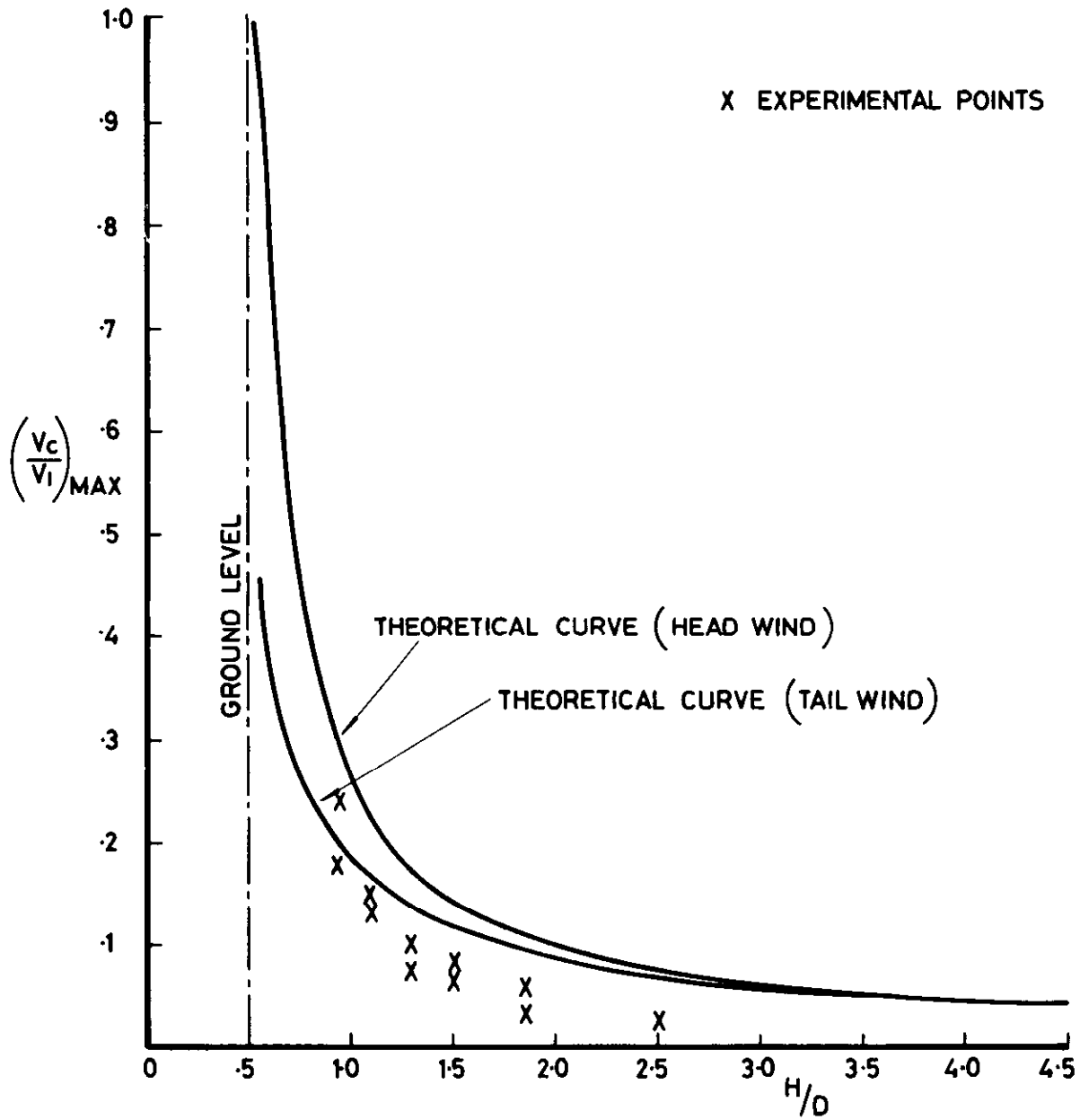


FIG.14 THEORETICAL MAXIMUM  $\frac{V_c}{V_i}$  FOR VARYING  $\frac{H}{D}$  RATIOS

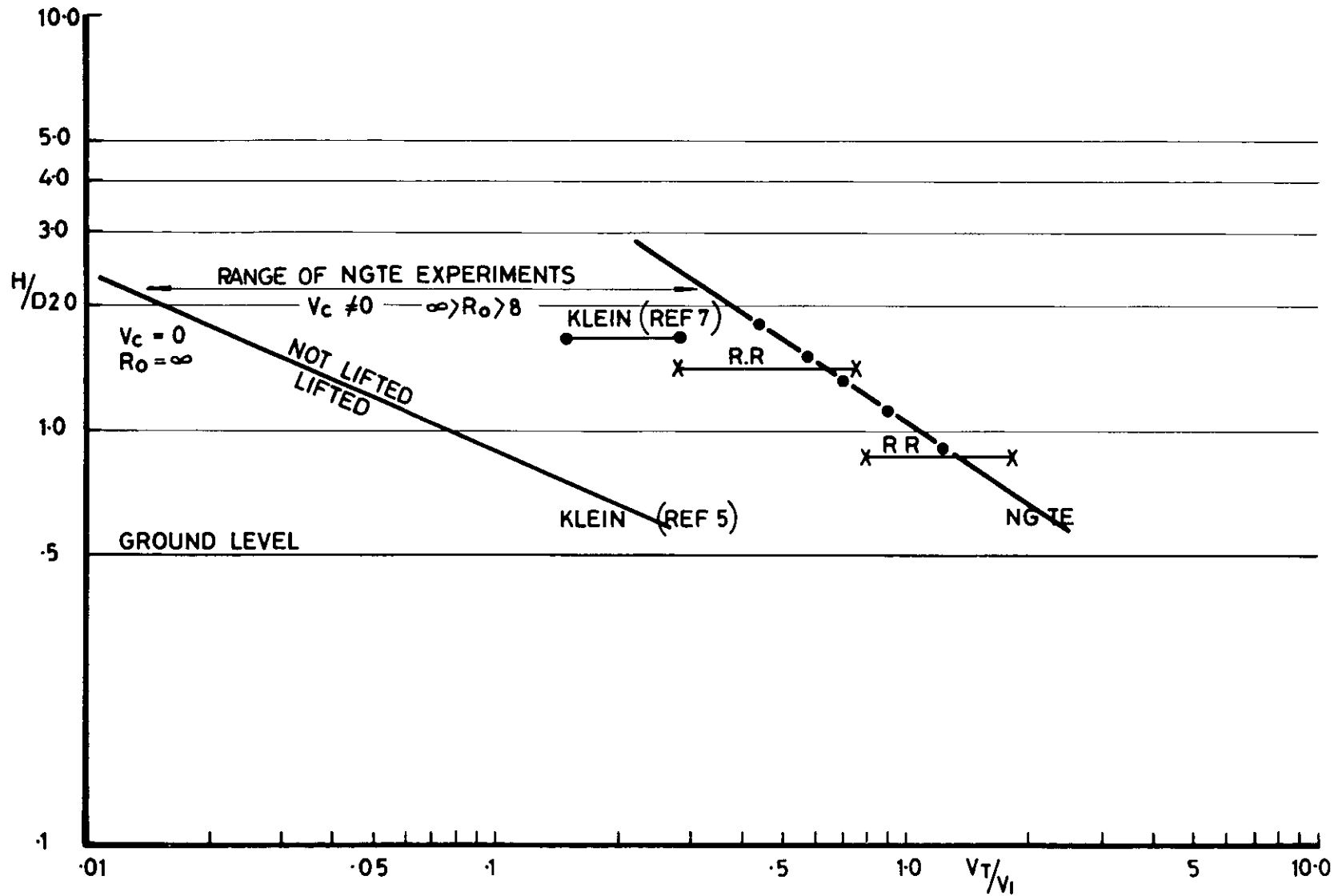


FIG.15 COMPARISON BETWEEN NGTE, ROLLS ROYCE AND DOUGLAS INGESTION ZONES  
 IN TERMS OF  $H/D$  AND  $V_t/V_i$

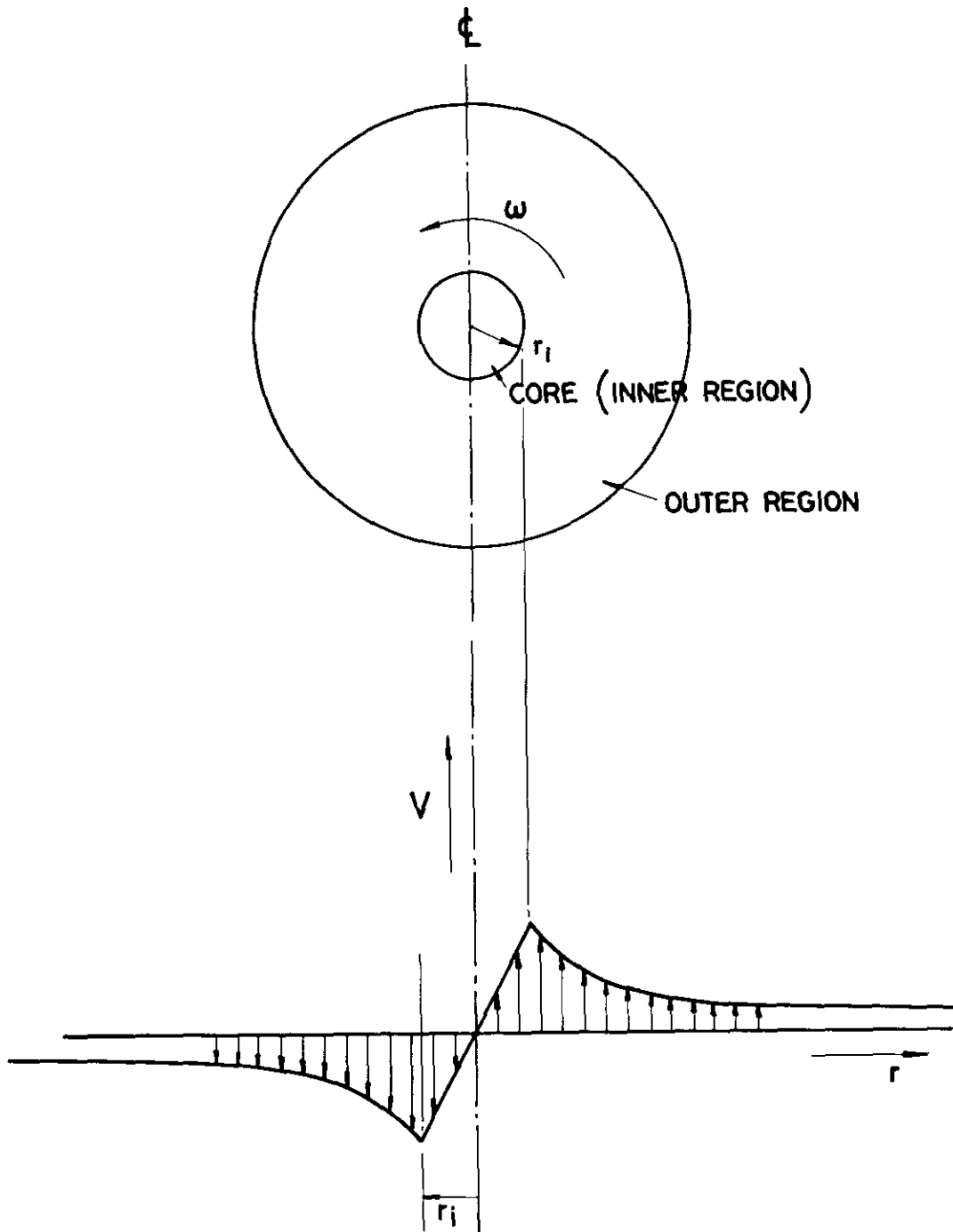


FIG.16 SIMPLIFIED VORTEX MODEL AND TYPICAL VELOCITY DISTRIBUTION

(REPRODUCED FROM PRANDTL & TIETJENS REF 10)

A.R.C. R & M 1114  
December 1968

621-757:533.697.2:532.527

Glenny, D. E.

INGESTION OF DEBRIS INTO INTAKES BY VORTEX ACTION

The impulsive lifting of particles over which the ground to intake vortex core passes is considered both theoretically and experimentally. Scaling laws are derived to relate model and full-scale tests and experimental evidence is cited to demonstrate their validity; it is further shown that for a given inlet velocity the strength of the vortex and the maximum size of particle that can be lifted is very much a function of the ambient vorticity and the strength of the wind blowing on to the intake.

Various methods of reducing ingestion were examined experimentally and although some reduced the frequency of ingestion none provided an

P.T.O.

A.R.C. R & M 1114  
December 1968

621-757:533.697.2:532.527

Glenny, D. E.

INGESTION OF DEBRIS INTO INTAKES BY VORTEX ACTION

The impulsive lifting of particles over which the ground to intake vortex core passes is considered both theoretically and experimentally. Scaling laws are derived to relate model and full-scale tests and experimental evidence is cited to demonstrate their validity; it is further shown that for a given inlet velocity the strength of the vortex and the maximum size of particle that can be lifted is very much a function of the ambient vorticity and the strength of the wind blowing on to the intake.

Various methods of reducing ingestion were examined experimentally and although some reduced the frequency of ingestion none provided an

P.T.O.

A.R.C. R & M 1114  
December 1968

621-757:533.697.2:532.527

Glenny, D. E.

INGESTION OF DEBRIS INTO INTAKES BY VORTEX ACTION

The impulsive lifting of particles over which the ground to intake vortex core passes is considered both theoretically and experimentally. Scaling laws are derived to relate model and full-scale tests and experimental evidence is cited to demonstrate their validity; it is further shown that for a given inlet velocity the strength of the vortex and the maximum size of particle that can be lifted is very much a function of the ambient vorticity and the strength of the wind blowing on to the intake.

Various methods of reducing ingestion were examined experimentally and although some reduced the frequency of ingestion none provided an

P.T.O.

absolute safeguard. However an operational technique which might ease the ingestion problem, involving a progressive opening of the throttle as the aircraft initially accelerates, is suggested.

absolute safeguard. However an operational technique which might ease the ingestion problem, involving a progressive opening of the throttle as the aircraft initially accelerates, is suggested.

absolute safeguard. However an operational technique which might ease the ingestion problem, involving a progressive opening of the throttle as the aircraft initially accelerates, is suggested.





© *Crown copyright 1970*

Printed and published by  
HER MAJESTY'S STATIONERY OFFICE

To be purchased from  
49 High Holborn, London WC1  
13a Castle Street, Edinburgh EH2 3AR  
109 St Mary Street, Cardiff CF1 1JW  
Brazennose Street, Manchester M60 8AS  
50 Fairfax Street, Bristol BS1 3DE  
258 Broad Street, Birmingham 1  
7 Linenhall Street, Belfast BT2 8AY  
or through any bookseller

*Printed in England*